

Supporting Information

Interrupted Helical Structure of Grafted Polypeptides in Brush-like Macromolecules

Jing Wang¹, Hua Lu², Yuan Ren¹, Yanfeng Zhang², Martha Morton³, Jianjun Cheng^{2}, Yao Lin^{1,3*}*

¹Polymer Program, Institute of Materials Science, University of Connecticut, Storrs, CT 06269,
USA;

²Department of Materials Science and Engineering, University of Illinois at Urbana-Champaign,
Urbana, IL 61801; USA,

³Department of Chemistry, University of Connecticut, Storrs, CT 06269, USA;

E-mail: ylin@ims.uconn.edu; jianjunc@uiuc.edu

Supplementary Figures

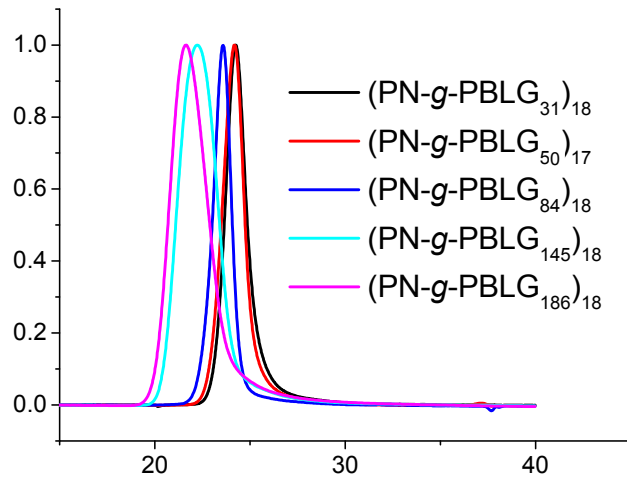


Figure S1 Overlay of the GPC curves (reflective index signal) of the $(\text{PN}-g\text{-PBLG}_n)_x$.

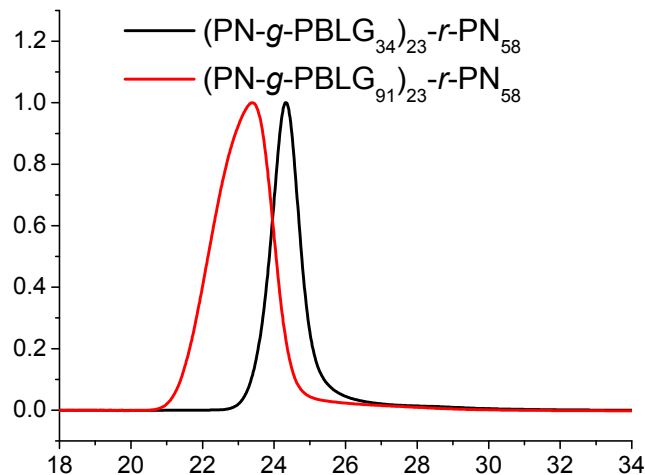


Figure S2 Overlay of the GPC curves (reflective index signal) of the $(\text{PN}-g\text{-PBLG}_{34})_{23}-r\text{-PN}_{58}$ and $(\text{PN}-g\text{-PBLG}_{91})_{23}-r\text{-PN}_{58}$.

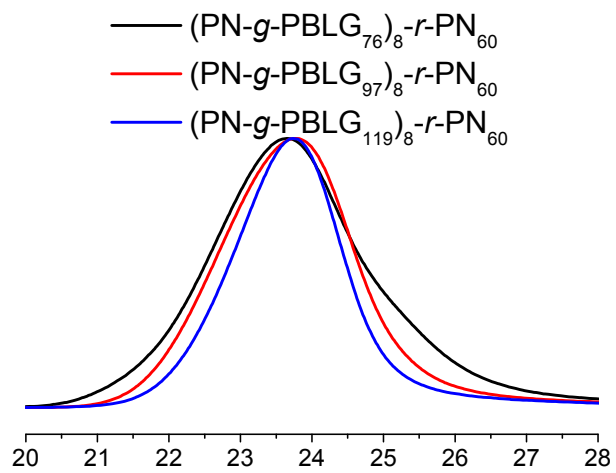


Figure S3 Overlay of the GPC curves (reflective index signal) of the $(\text{PN-}g\text{-PBLG}_{76})_8\text{-}r\text{-}\text{PN}_{60}$, $(\text{PN-}g\text{-PBLG}_{97})_8\text{-}r\text{-}\text{PN}_{60}$ and $(\text{PN-}g\text{-PBLG}_{119})_8\text{-}r\text{-}\text{PN}_{60}$.

TFA induced helix-to-coil transitions studies for PBLG-containing polymers (Figure S4-S18). Solvent induced helix-coil transition studies were carried out on a Bruker DRX 500 MHz spectrometer, using premeasured compositions of TFA-*d* and CDCl₃ as the solvent. In the studies, at least 2 % TFA-*d* has been added into the solution to prevent the potential aggregation of PBLG chains to form helix bundles. We adapted the method from Goodman and Marborough¹ to follow TFA-*d* induced helix-coil transition of PBLGs. The following figures show representative spectra of PBLG containing macromolecules at different solvent compositions at 298 K. The chemical shifts at 4.0 ppm and 4.6 ppm are used to identify the α -helix and random coil structures, respectively. The fraction of α -CH existing in α -helix structure was used to calculate the helical contents of PBLGs at a given solvent composition. On increasing the volume fraction of TFA in the CDCl₃/TFA-*d* mixture, the α -helix conformation in homo-PBLGs diminishes and eventually disappears, as can be seen from the reduced intensity of α -CH peak at 4.0 ppm. This solvent induced helix-coil transition is more apparent when plotting the helix contents of PBLGs as a function of volume fraction of TFA added in the solution.

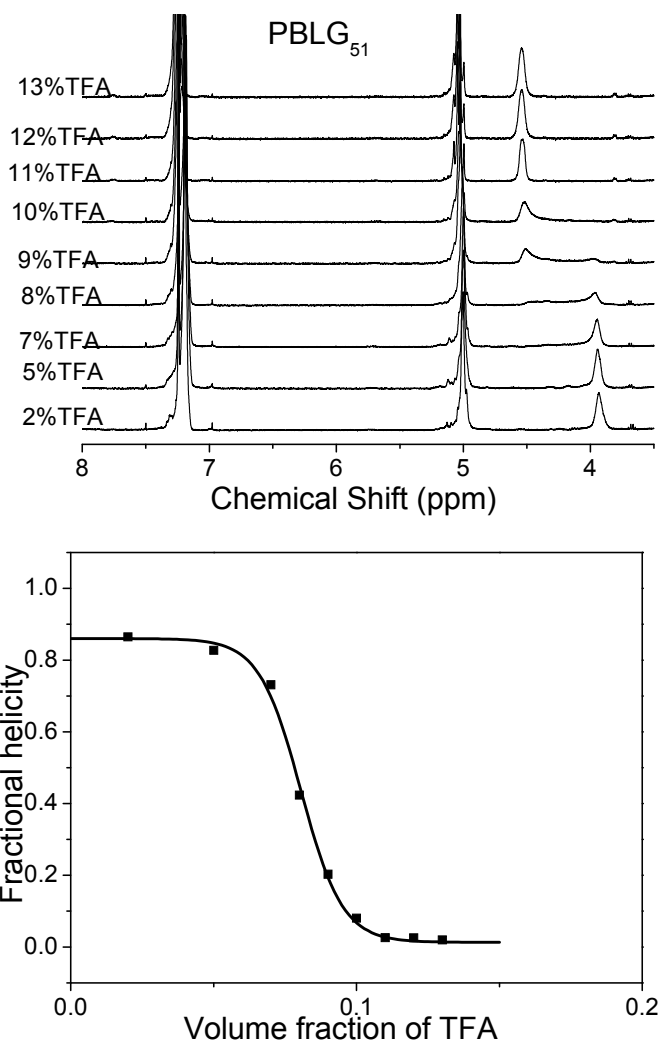


Figure S4 ^1H NMR spectra of TFA induced helix-to-coil transition of PBLG₅₁ in TFA-*d*/CDCl₃ mixture. The concentration of Glu residues is 0.01M.

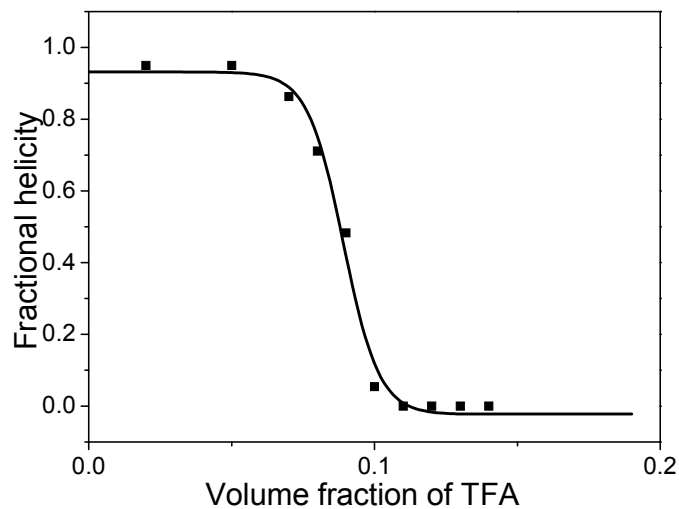
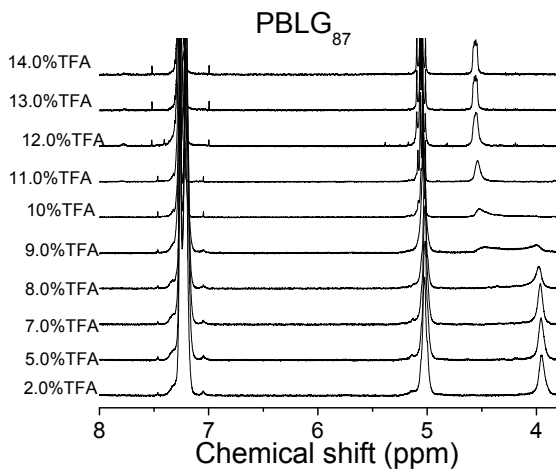


Figure S5 ^1H NMR spectra of TFA induced helix-to-coil transition of PBLG₈₇ in TFA-*d*/CDCl₃ mixture. The concentration of Glu residues is 0.01M.

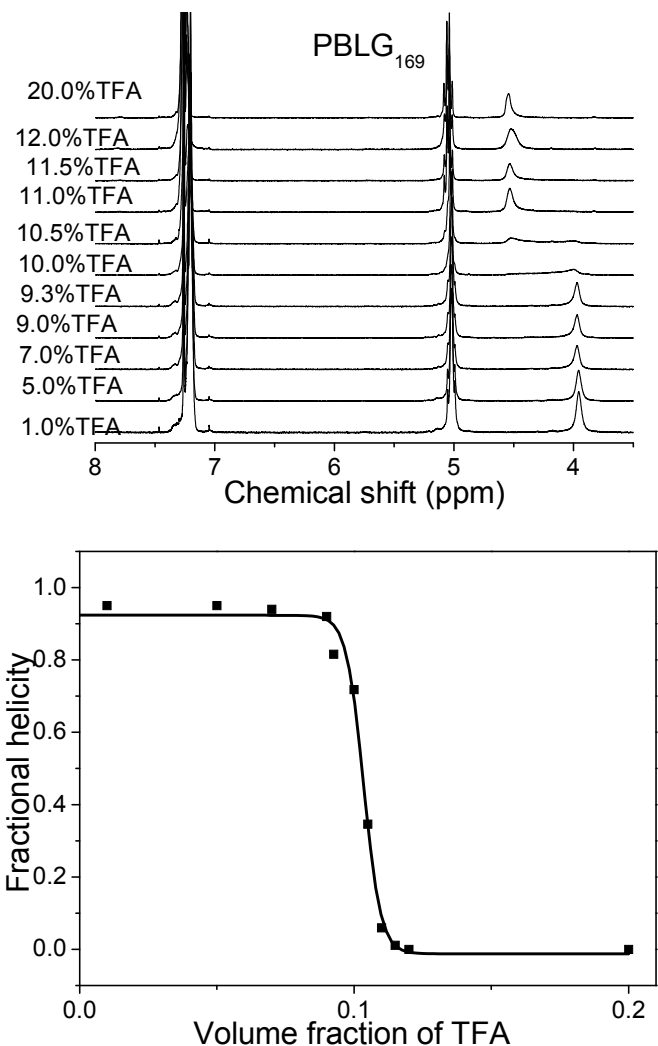


Figure S6 ¹H NMR spectra of TFA induced helix-to-coil transition of PBLG₁₆₉ in TFA-*d*/CDCl₃ mixture. The concentration of Glu residues is 0.01M.

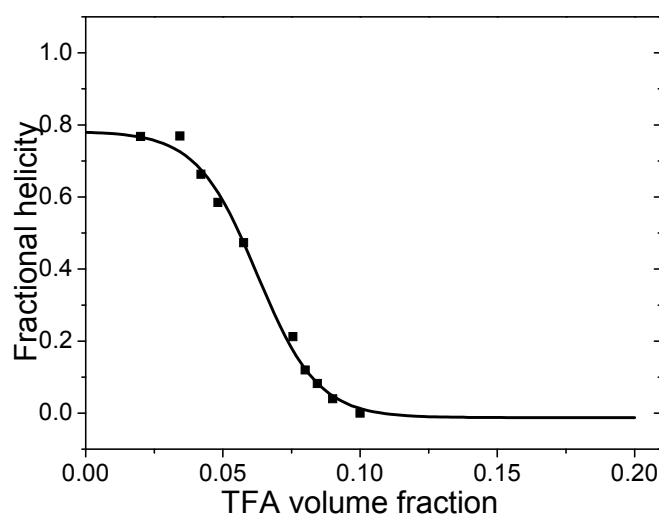
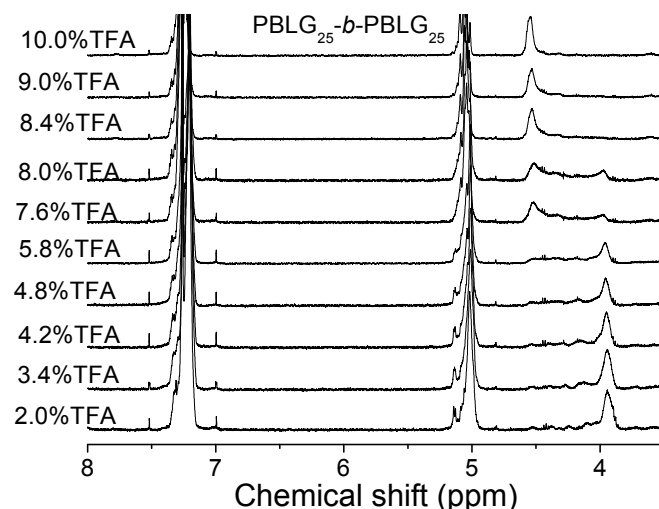


Figure S7 ^1H NMR spectra of TFA induced helix-to-coil transition of PBLG₂₅-*b*-PBLG₂₅ in TFA-*d*/CDCl₃ mixture. The concentration of Glu residues is 0.01M.

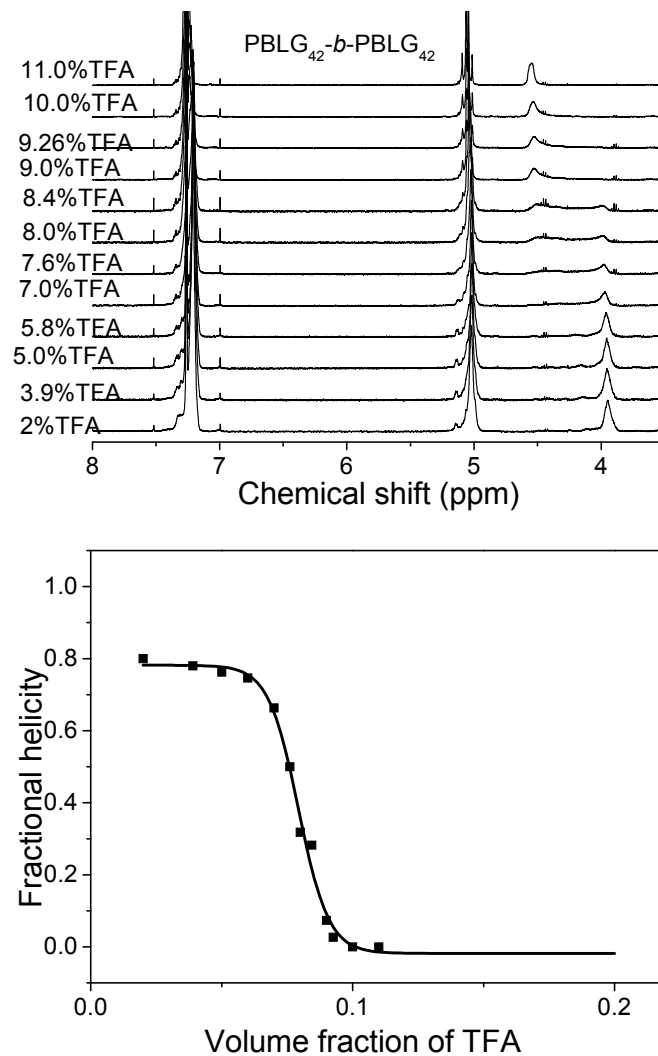


Figure S8 ¹H NMR spectra of TFA induced helix-to-coil transition of PBLG₄₂-*b*-PBLG₄₂ in TFA-*d*/CDCl₃ mixture. The concentration of Glu residues is 0.01M.

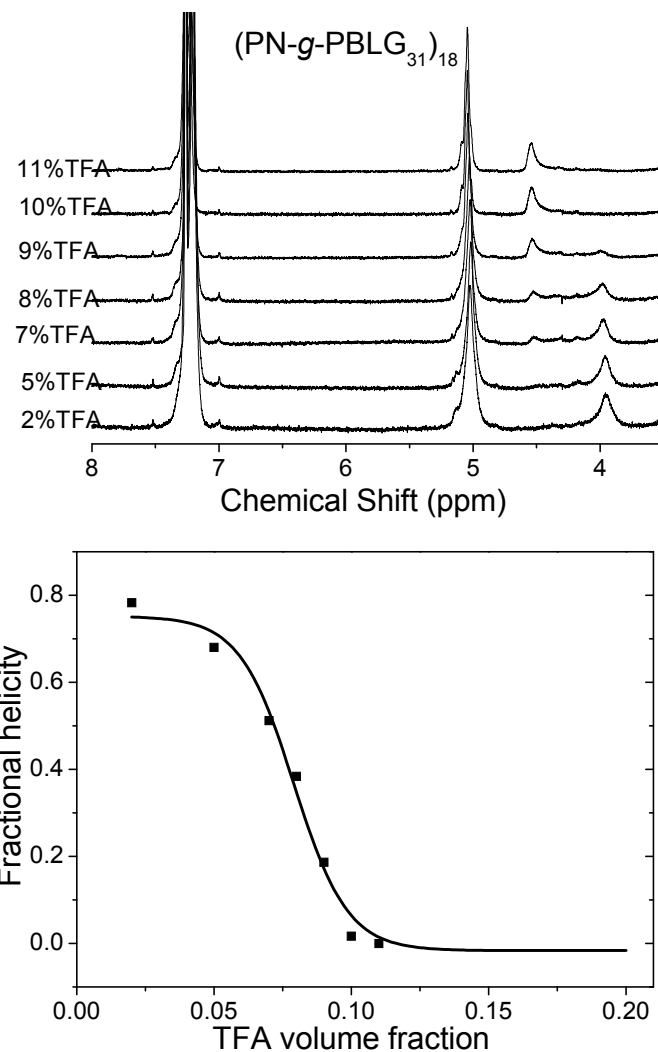


Figure S9 ¹H NMR spectra of TFA induced helix-to-coil transition of $(\text{PN}-g\text{-PBLG}_{31})_{18}$ in TFA-*d*/CDCl₃ mixture. The concentration of Glu residues is 0.01M.

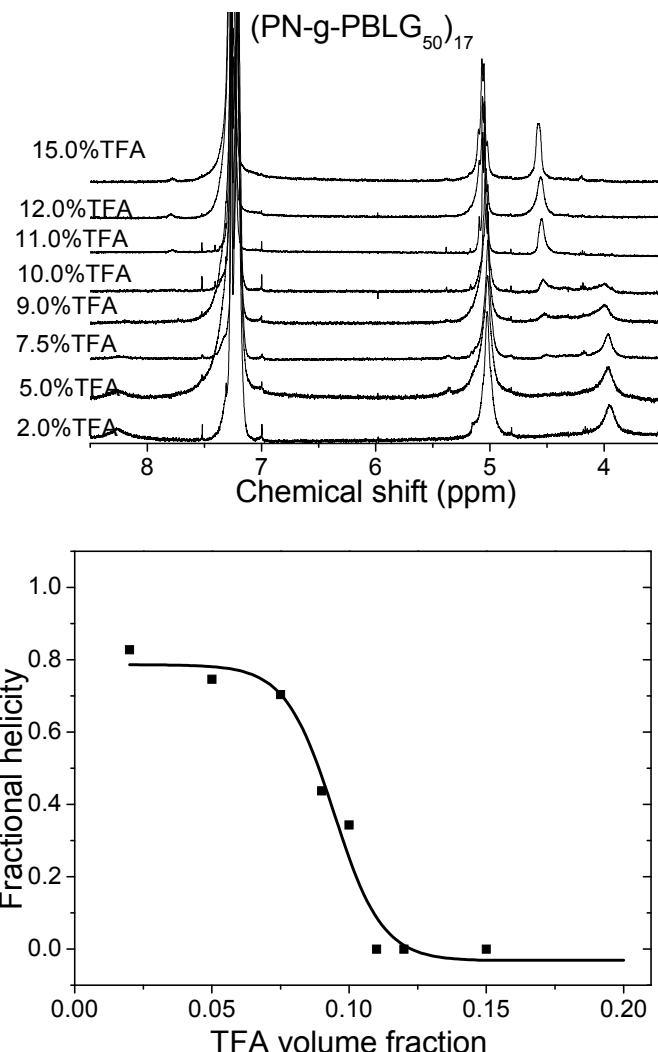


Figure S10 ¹H NMR spectra of TFA induced helix-to-coil transition of (PN-g-PBLG₅₀)₁₇ in TFA-d/CDCl₃ mixture. The concentration of Glu residues is 0.01M.

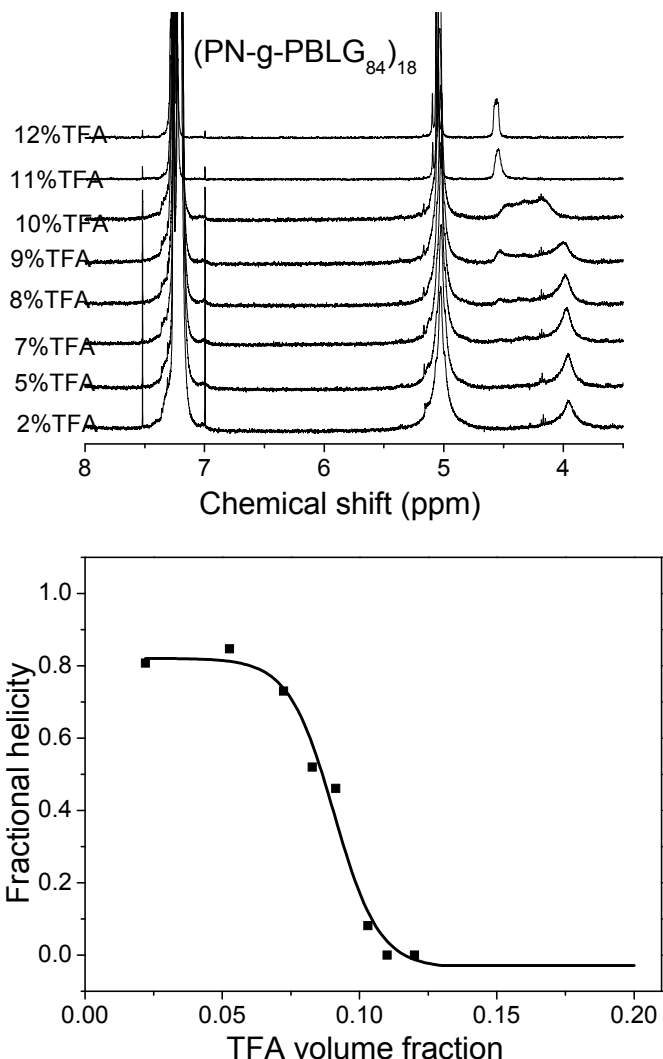


Figure S11 ¹H NMR spectra of TFA induced helix-to-coil transition of (PN-g-PBLG₈₄)₁₈ in TFA-d/CDCl₃ mixture. The concentration of Glu residues is 0.01M.

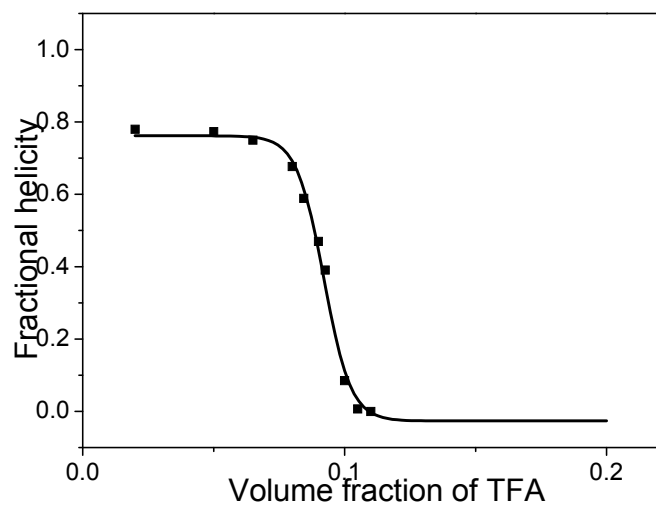
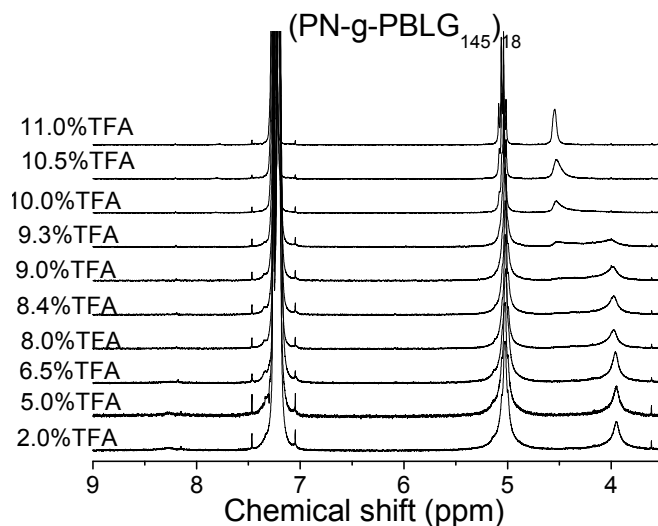


Figure S12 ^1H NMR spectra of TFA induced helix-to-coil transition of $(\text{PN-g-PBLG}_{145})_{18}$ in $\text{TFA}-d/\text{CDCl}_3$ mixture. The concentration of Glu residues is 0.01M.

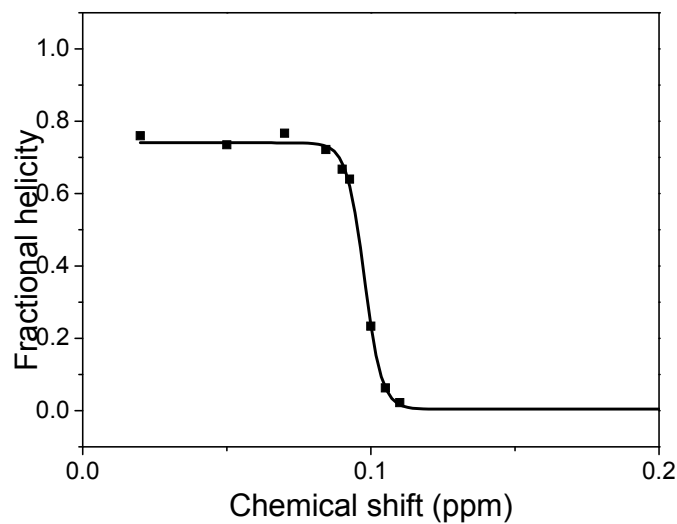
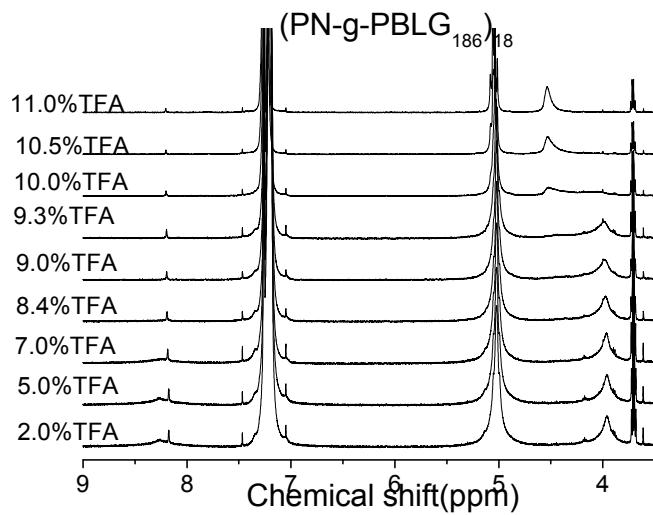


Figure S13 ^1H NMR spectra of TFA induced helix-to-coil transition of $(\text{PN-g-PBLG}_{186})_{18}$ in $\text{TFA}-d/\text{CDCl}_3$ mixture. The concentration of Glu residues is 0.01M.

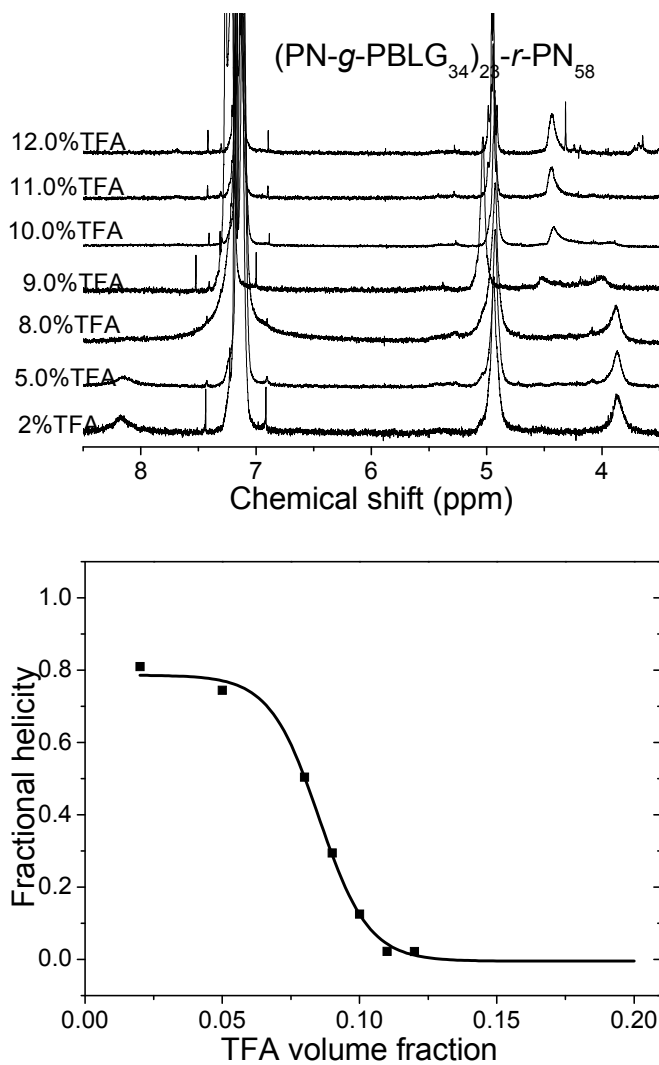


Figure S14 ¹H NMR spectra of TFA induced helix-to-coil transition of (PN-g-PBLG₃₄)₂₃-r-PN₅₈ in TFA-d/CDCl₃ mixture. The concentration of Glu residues is 0.01M.

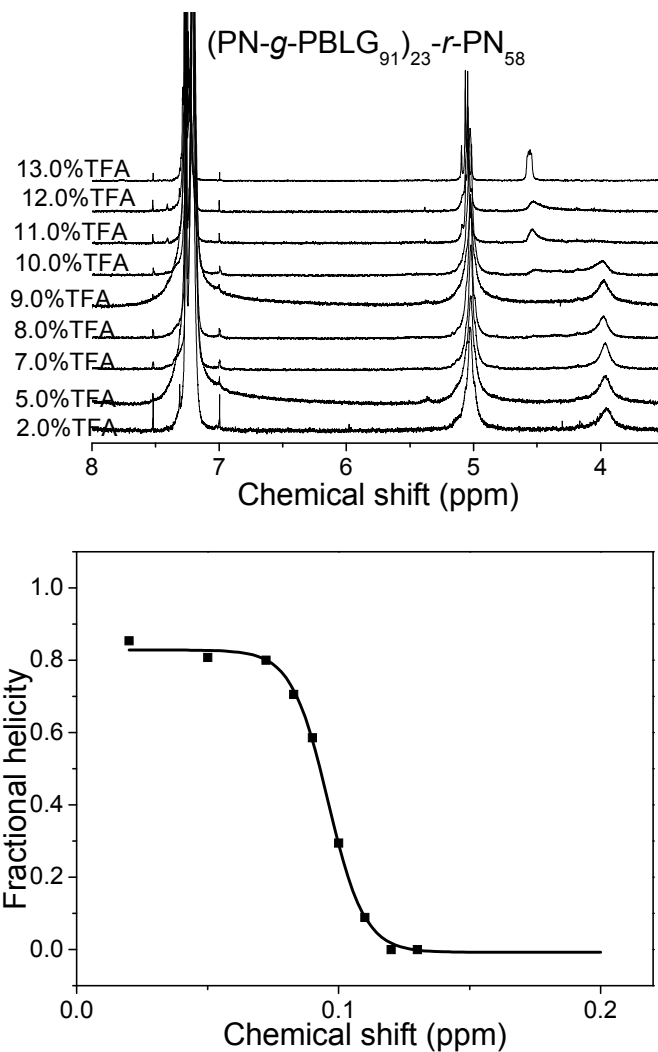


Figure S15 ^1H NMR spectra of TFA induced helix-to-coil transition of $(\text{PN}-g\text{-PBLG}_{91})_{23}-r\text{-PN}_{58}$ in $\text{TFA-}d/\text{CDCl}_3$ mixture. The concentration of Glu residues is 0.01M.

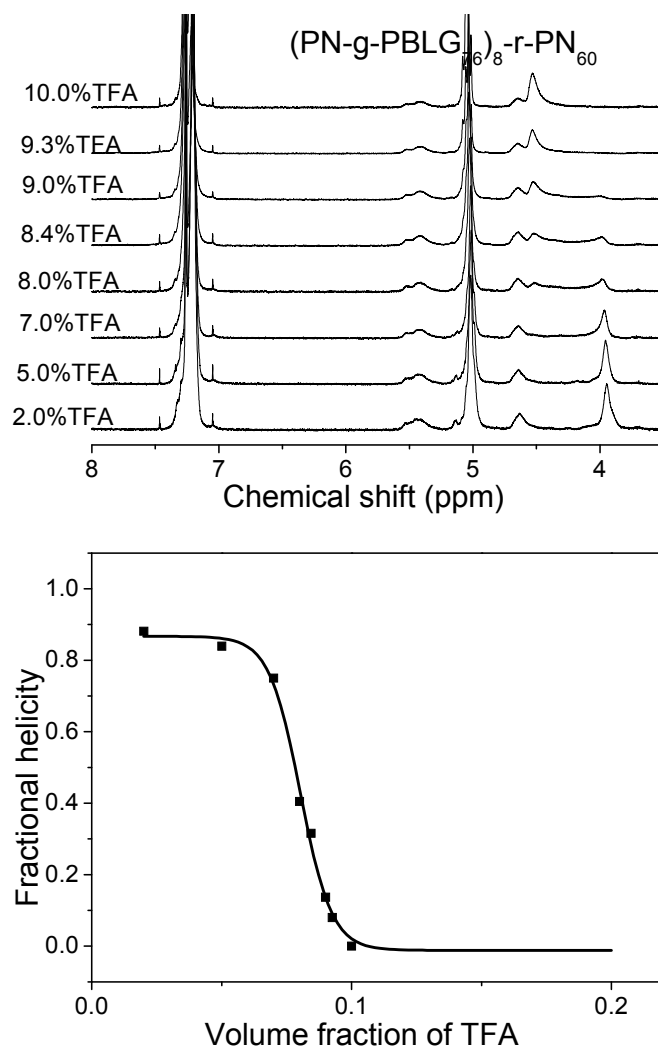


Figure S16 ¹H NMR spectra of TFA induced helix-to-coil transition of $(\text{PN-g-PBLG}_{76})_8\text{-r-PN}_{60}$ in TFA-*d*/CDCl₃ mixture. The concentration of Glu residues is 0.01M.

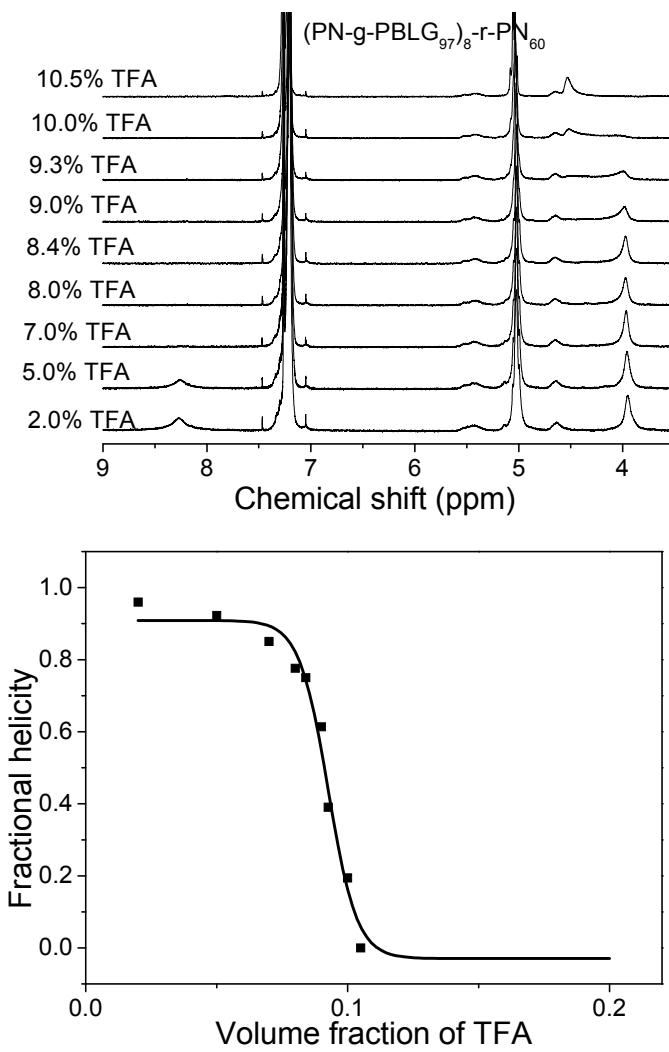


Figure S17 ¹H NMR spectra of TFA induced helix-to-coil transition of $(\text{PN-g-PBLG}_{97})_8\text{-r-PN}_{60}$ in TFA-*d*/CDCl₃ mixture. The concentration of Glu residues is 0.01M.

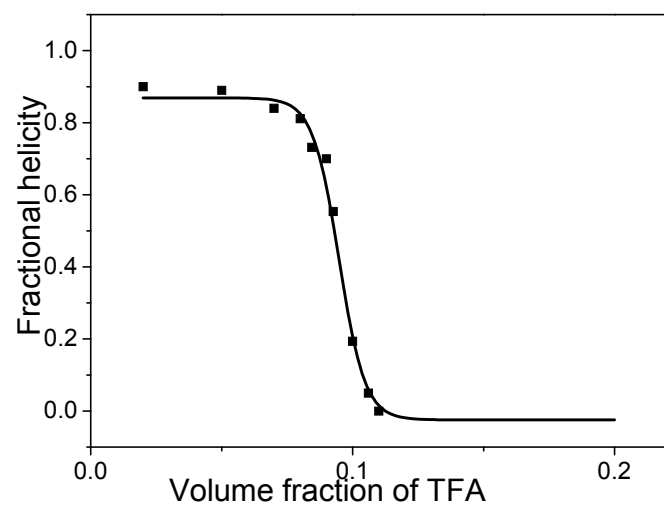
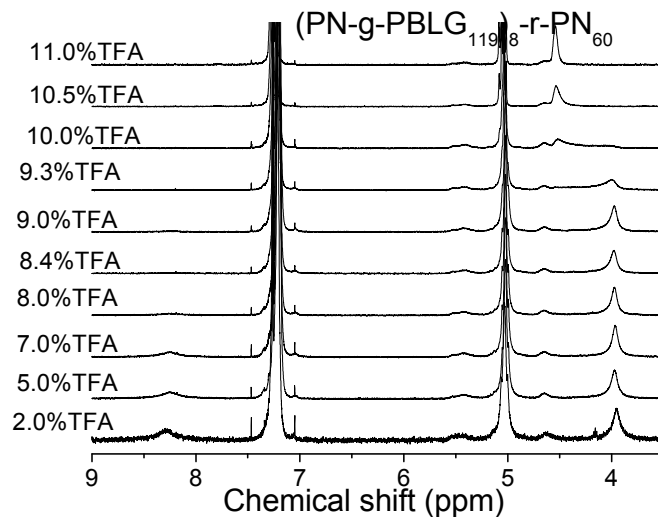


Figure S18 ^1H NMR spectra of TFA induced helix-to-coil transition of $(\text{PN-g-PBLG}_{119})_8\text{-r-PN}_{60}$ in $\text{TFA-}d/\text{CDCl}_3$ mixture. The concentration of Glu residues is 0.01M.

NOESY study of different polymers (Figure S19-S22). Polymers for NOESY experiments were dissolved in 98:2 *d*-CDCl₃:*d*-TFA and sealed in NMR tubes to prevent solvent evaporation. 2D NOESY experiments were performed on a Bruke DRX-500 MHz spectrometer with the $(\pi/2)-t_1-(\pi/2)-\tau_m-(\pi/2)-t_2$ pulse sequence. 2048K spectra were acquired with a sweep width of 6510 Hz in each dimension. The $\pi/2$ pulse width was 8.4 μ s, τ_m was 100 ms, and the delay between acquisitions was 2 s.

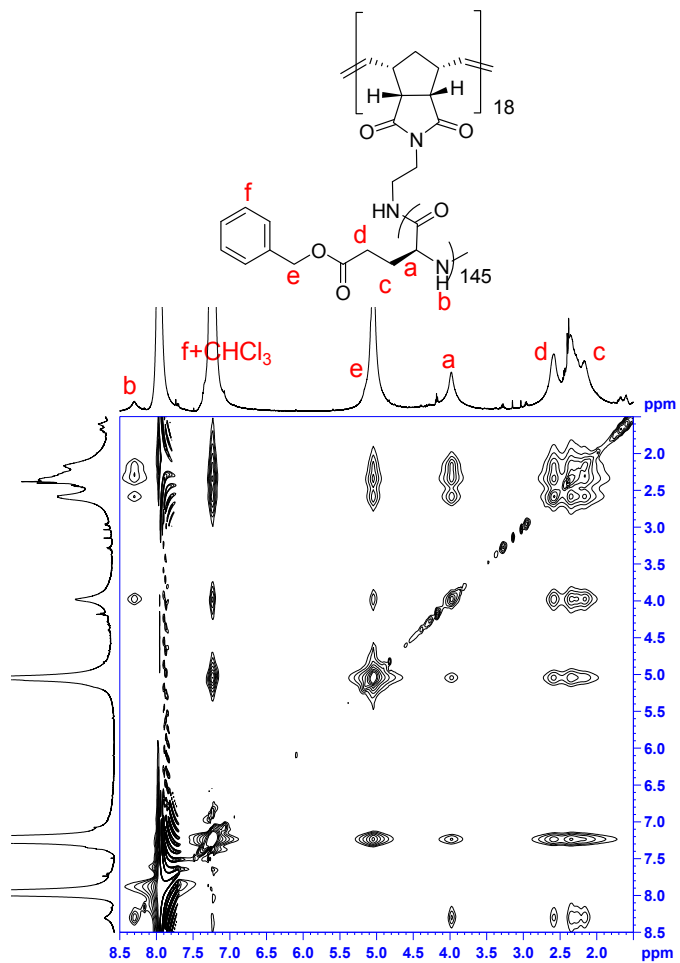


Figure S19. The NOESY spectrum of (PN-g-PBLG₁₄₅)₁₈ obtained by using the $(\pi/2)-t_1-(\pi/2)-\tau_m-(\pi/2)-t_2$ pulse sequence.

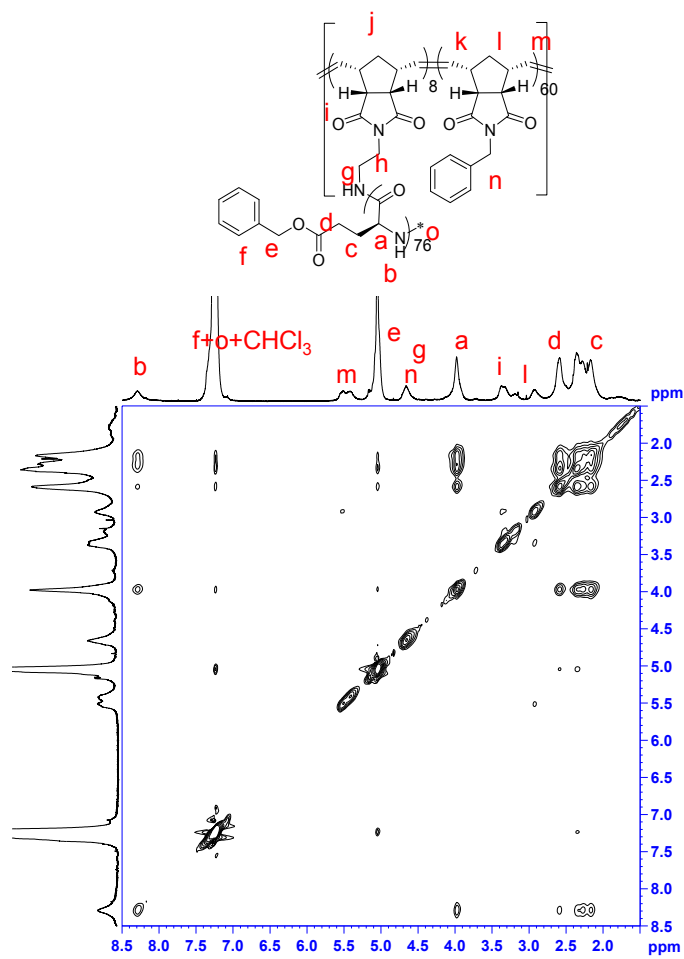


Figure S20. The NOESY spectrum of (PN-g-PBLG₇₆)₈-r-PN₆₀ obtained by using the $(\pi/2)$ - t_1 - $(\pi/2)$ - τ_m - $(\pi/2)$ - t_2 pulse sequence.

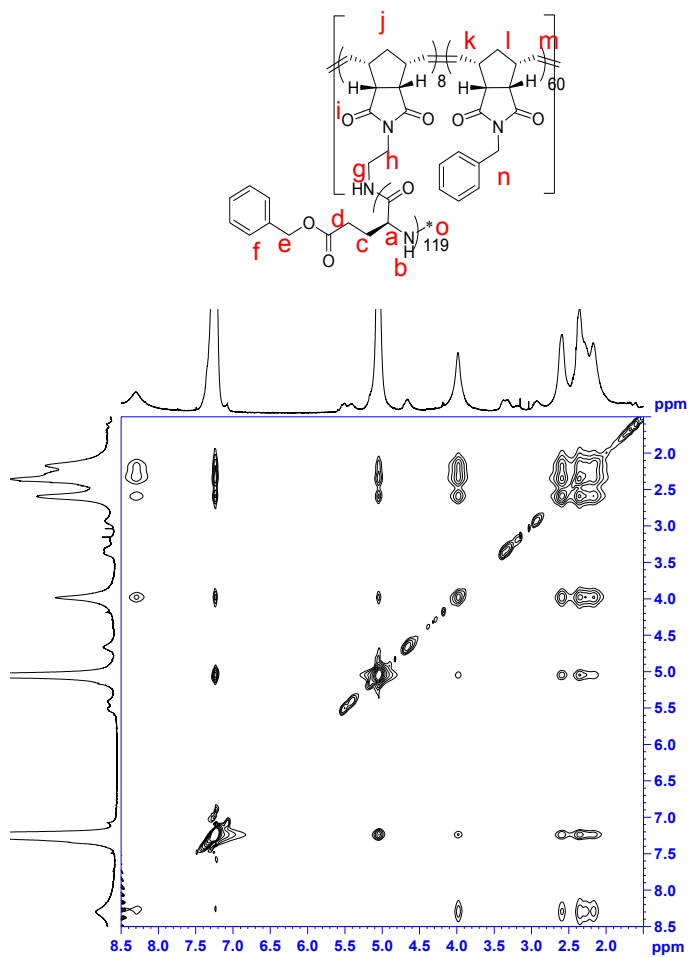


Figure S21. The NOESY spectrum of (PN-g-PBLG₁₁₉)₈-r-PN₆₀ obtained by using the $(\pi/2)$ - t_1 - $(\pi/2)$ - τ_m - $(\pi/2)$ - t_2 pulse sequence.

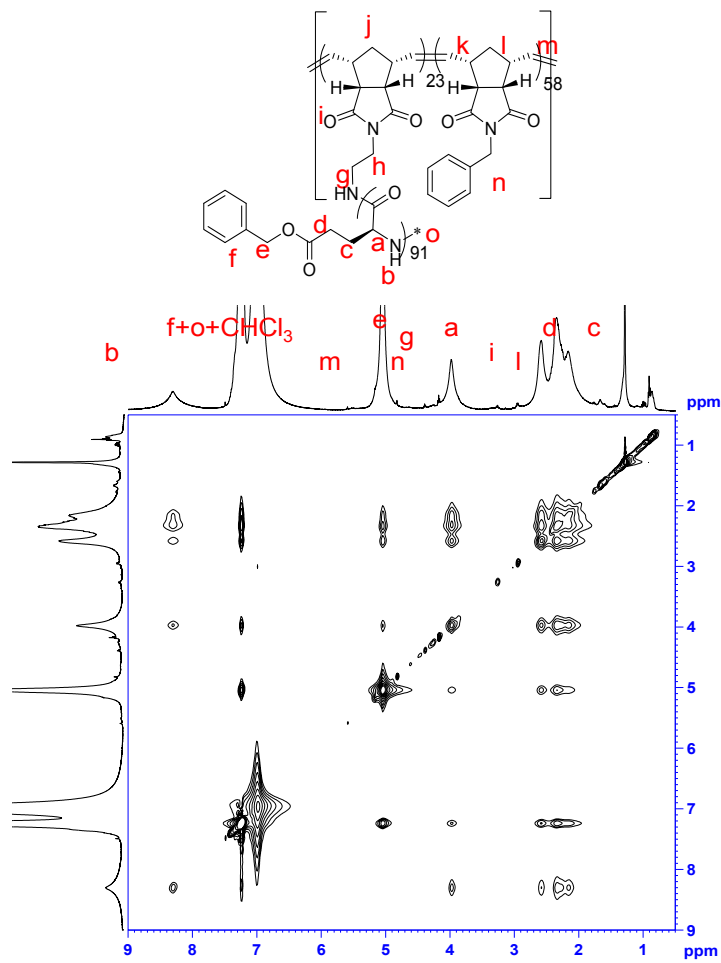


Figure S22. The NOESY spectrum of $(\text{PN-g-PBLG}_{91})_{23}-r-\text{PN}_{58}$ obtained by using the $(\pi/2)-t_1-(\pi/2)-\tau_m-(\pi/2)-t_2$ pulse sequence.

TFA induced helix-to-coil transition studies for PZLL-containing polymers (Figure S23-S31). The experimental procedure is the same as described for the study on PBLG-containing polymers.

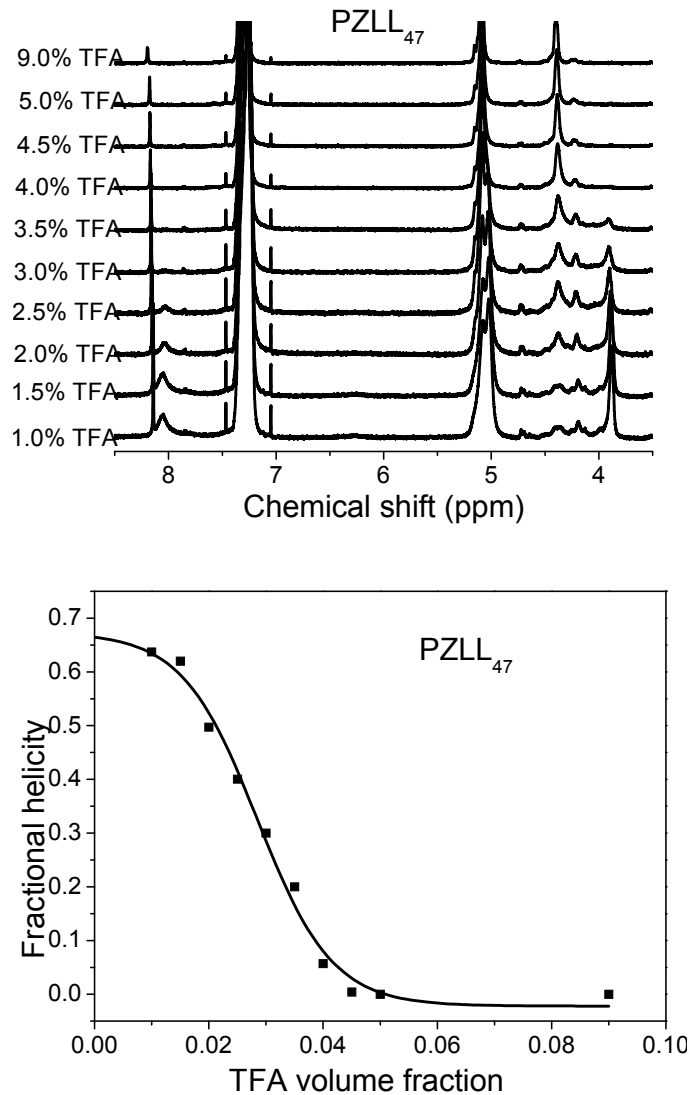


Figure S23 ^1H NMR spectra of TFA induced helix-to-coil transition of PZLL_{47} in $\text{TFA-}d/\text{CDCl}_3$ mixture. The concentration of Lys residues is 0.01M.

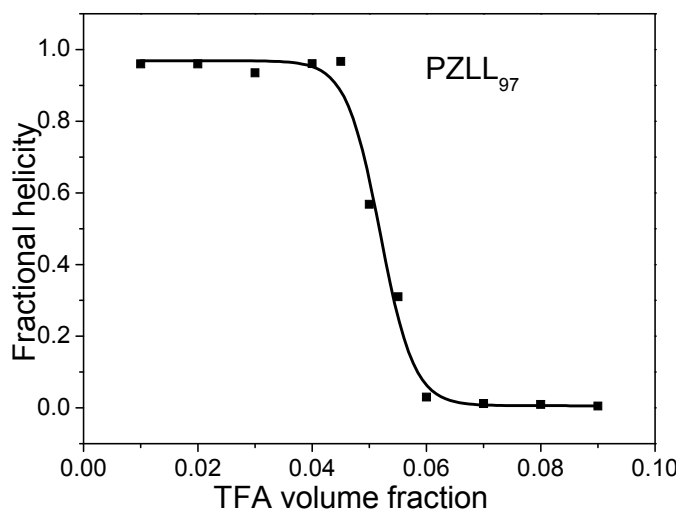
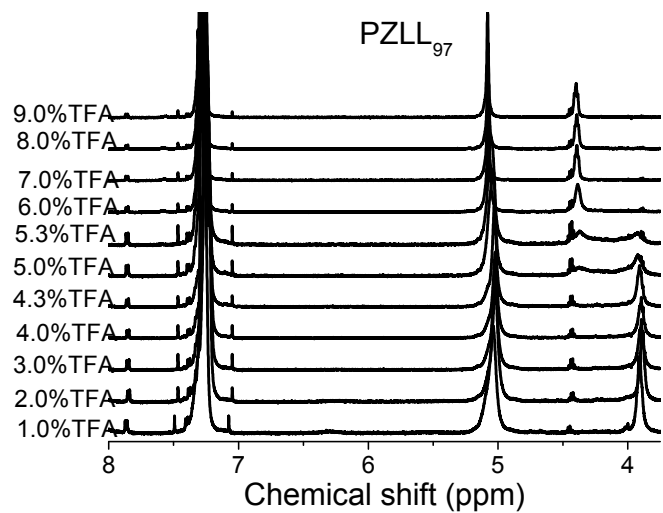


Figure S24 ^1H NMR spectra of TFA induced helix-to-coil transition of PZLL₉₇ in TFA-d/CDCl₃ mixture. The concentration of Lys residues is 0.01M.

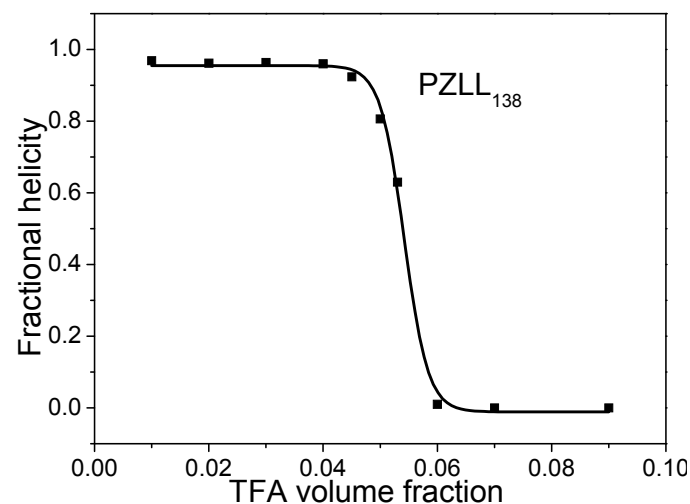
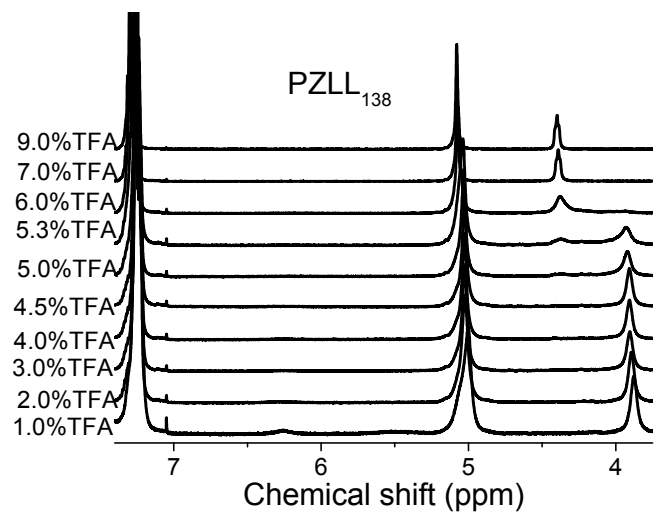


Figure S25 ^1H NMR spectra of TFA induced helix-to-coil transition of PZLL₁₃₈ in TFA-*d*/CDCl₃ mixture. The concentration of Lys residues is 0.01M.

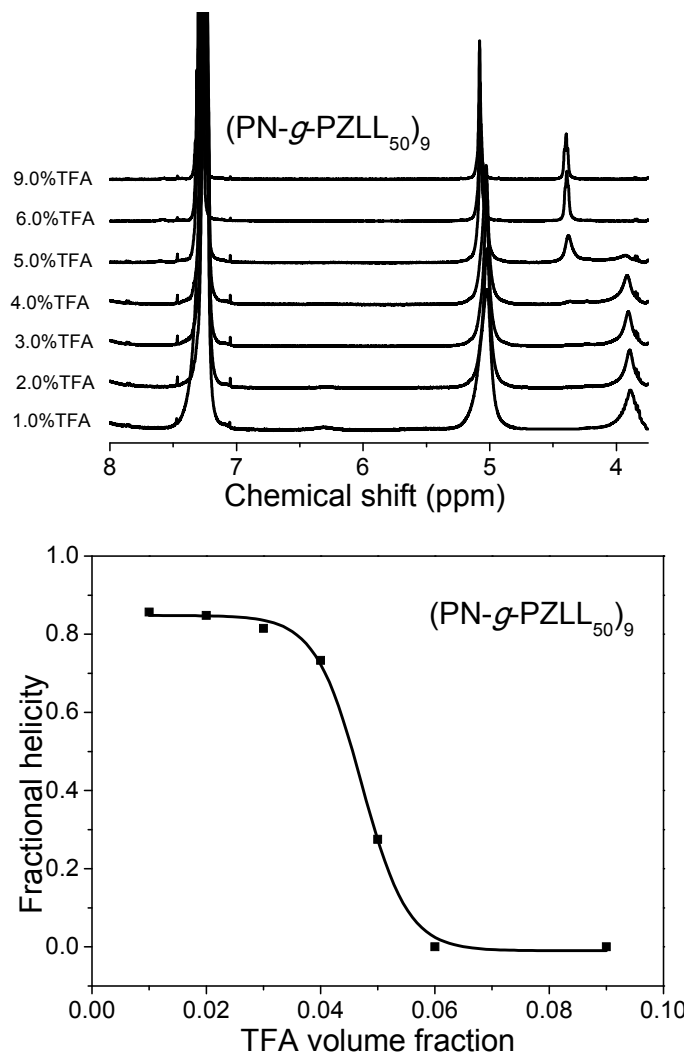


Figure S26 ^1H NMR spectra of TFA induced helix-to-coil transition of $(\text{PN}-g\text{-PZLL}_{50})_9$ in TFA- d/CDCl_3 mixture. The concentration of residues is 0.01M.

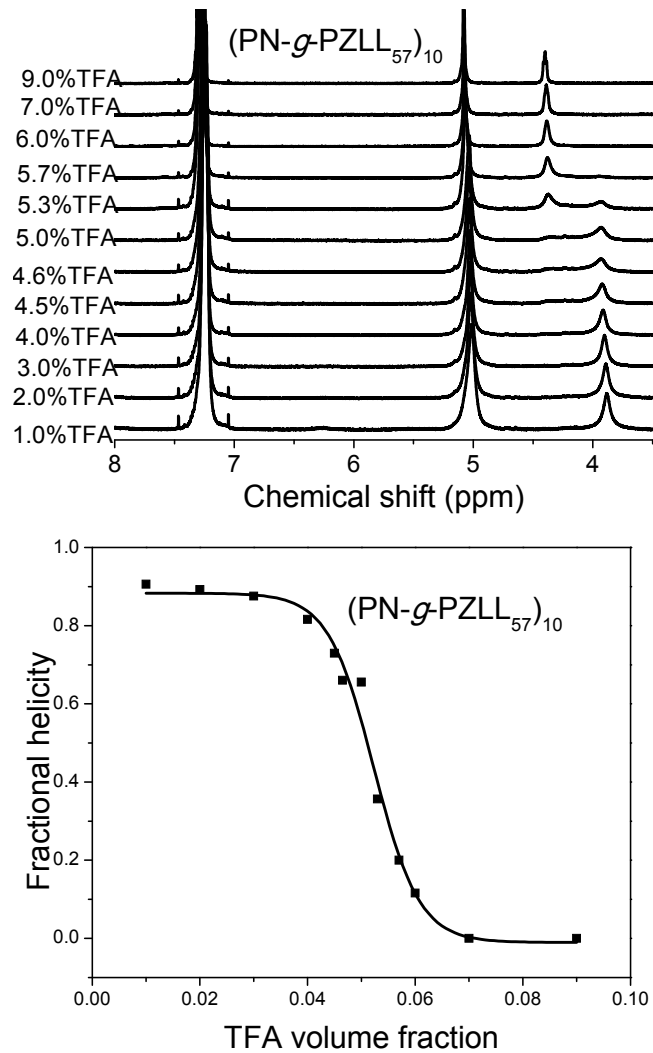


Figure S27 ^1H NMR spectra of TFA induced helix-to-coil transition of $(\text{PN-}g\text{-PZLL}_{57})_{10}$ in TFA-*d*/CDCl₃ mixture. The concentration of residues is 0.01M.

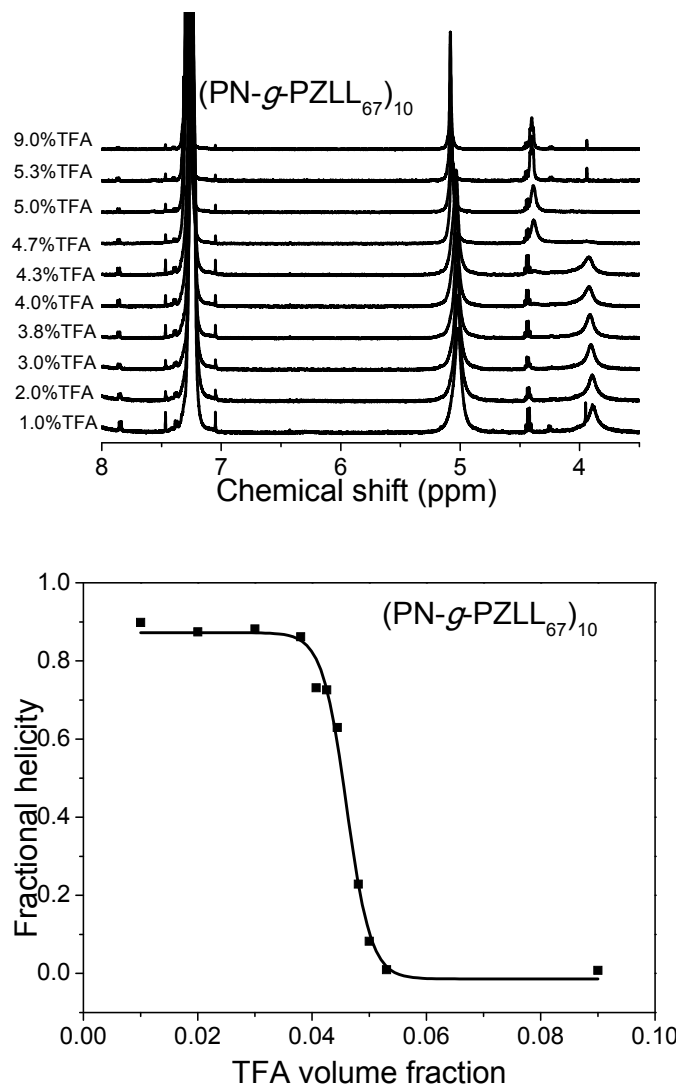


Figure S28 ¹H NMR spectra of TFA induced helix-to-coil transition of (PN-g-PZLL₆₇)₁₀ in TFA-d/CDCl₃ mixture. The concentration of residues is 0.01M.

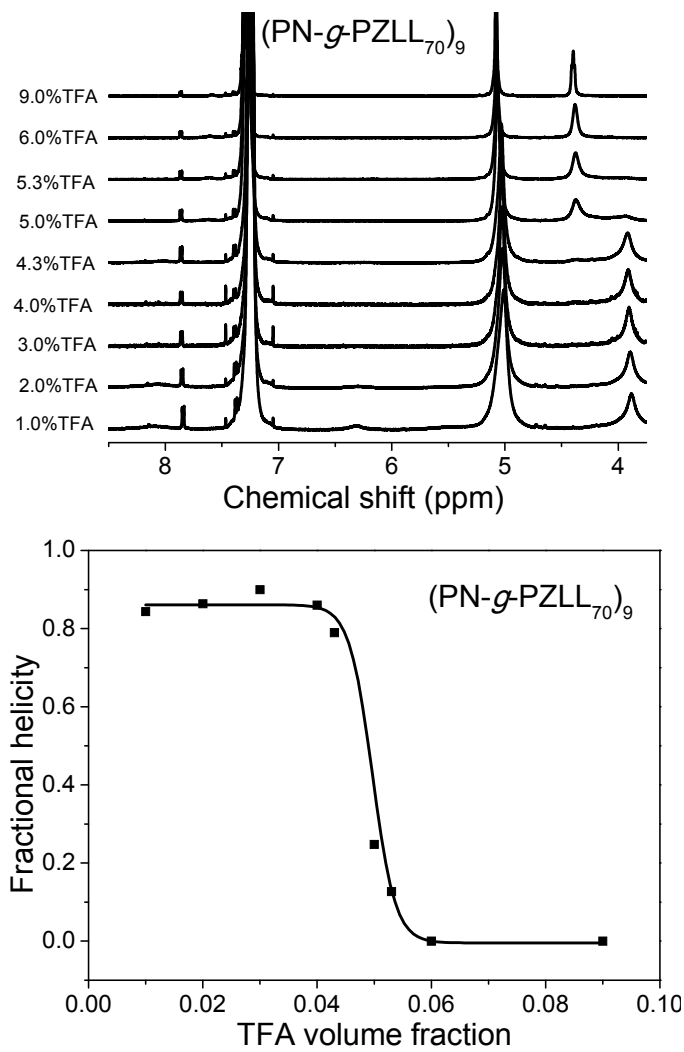


Figure S29 ¹H NMR spectra of TFA induced helix-to-coil transition of $(\text{PN-}g\text{-PZLL}_{70})_9$ in TFA-*d*/CDCl₃ mixture. The concentration of residues is 0.01M.

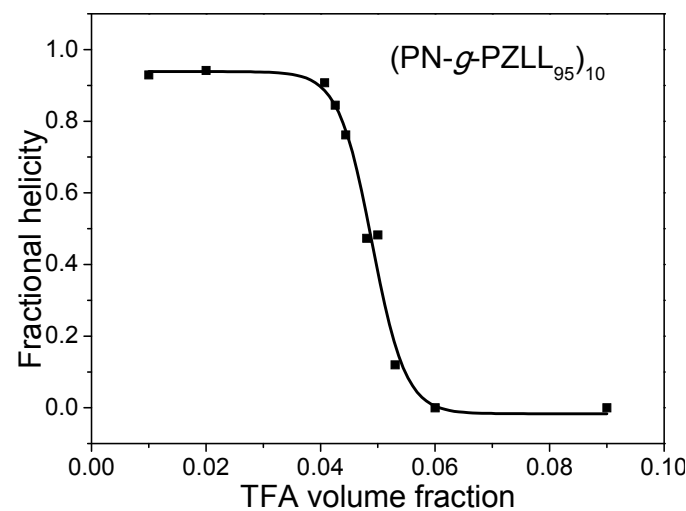
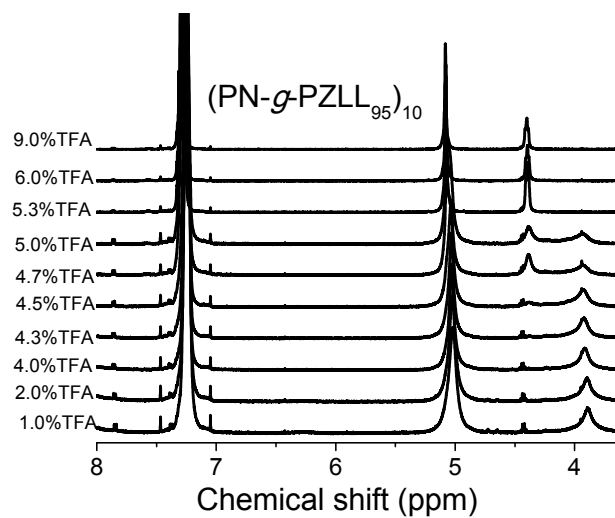


Figure S30 ^1H NMR spectra of TFA induced helix-to-coil transition of $(\text{PN-}g\text{-PZLL}_{95})_{10}$ in $\text{TFA-}d/\text{CDCl}_3$ mixture. The concentration of residues is 0.01M.

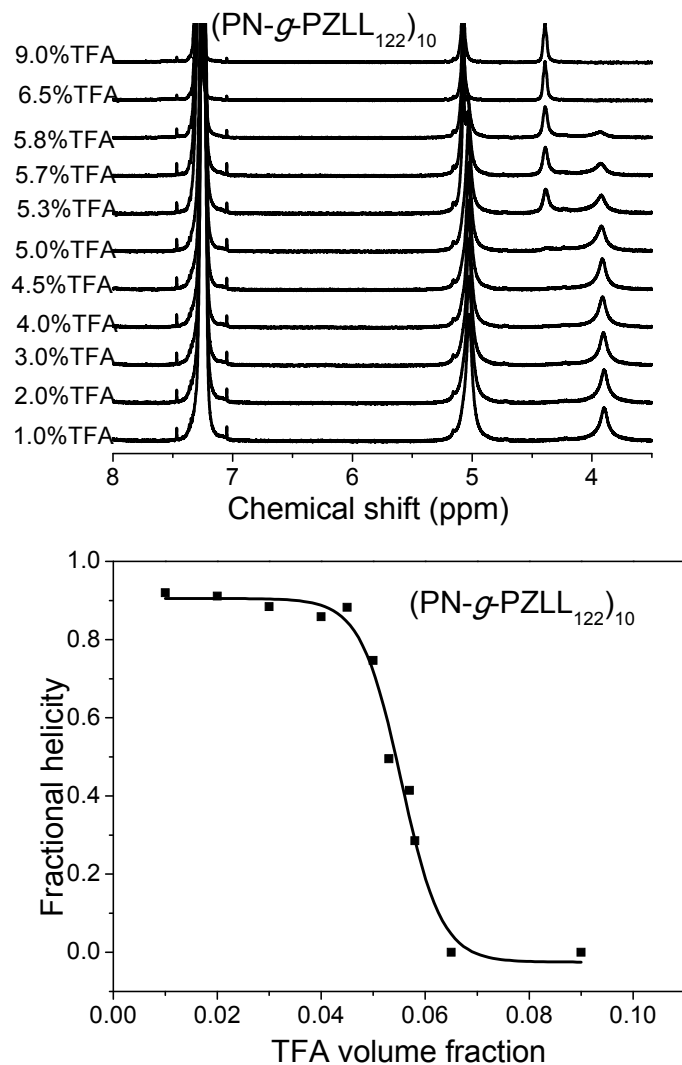


Figure S31 ¹H NMR spectra of TFA induced helix-to-coil transition of (PN-g-PZLL₁₂₂)₁₀ in TFA-*d*/CDCl₃ mixture. The concentration of residues is 0.01M.

NOESY study of PZLL-containing polymers (S32-38). The experimental procedure is the same as described for the studies on PBLG-containing polymers.

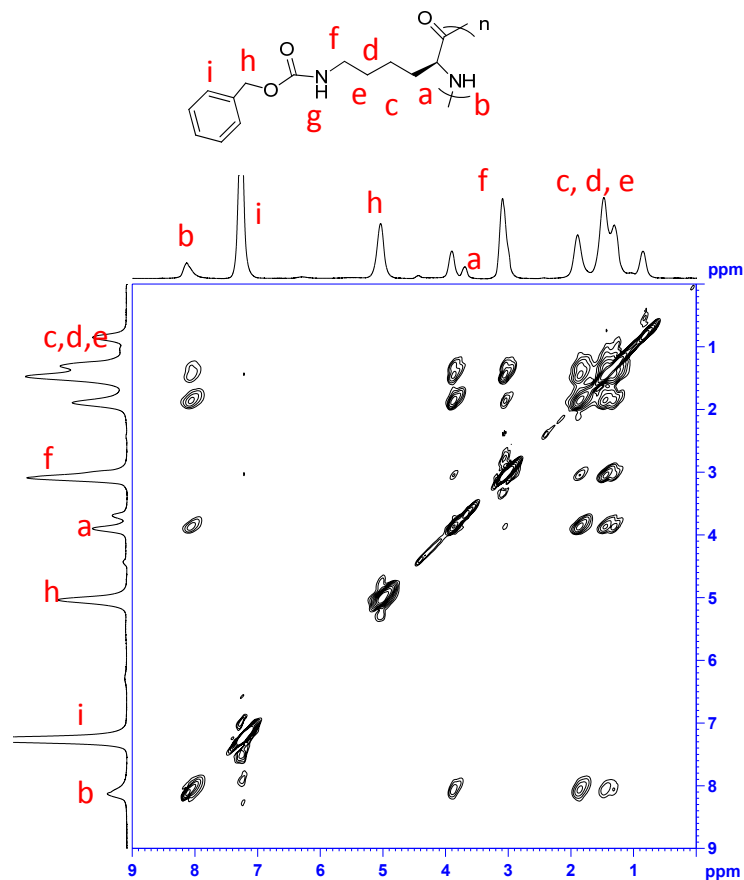


Figure S32. The NOESY spectrum of PZLL₉₇ obtained by using the $(\pi/2)-t_1-(\pi/2)-\tau_m-(\pi/2)-t_2$ pulse sequence.

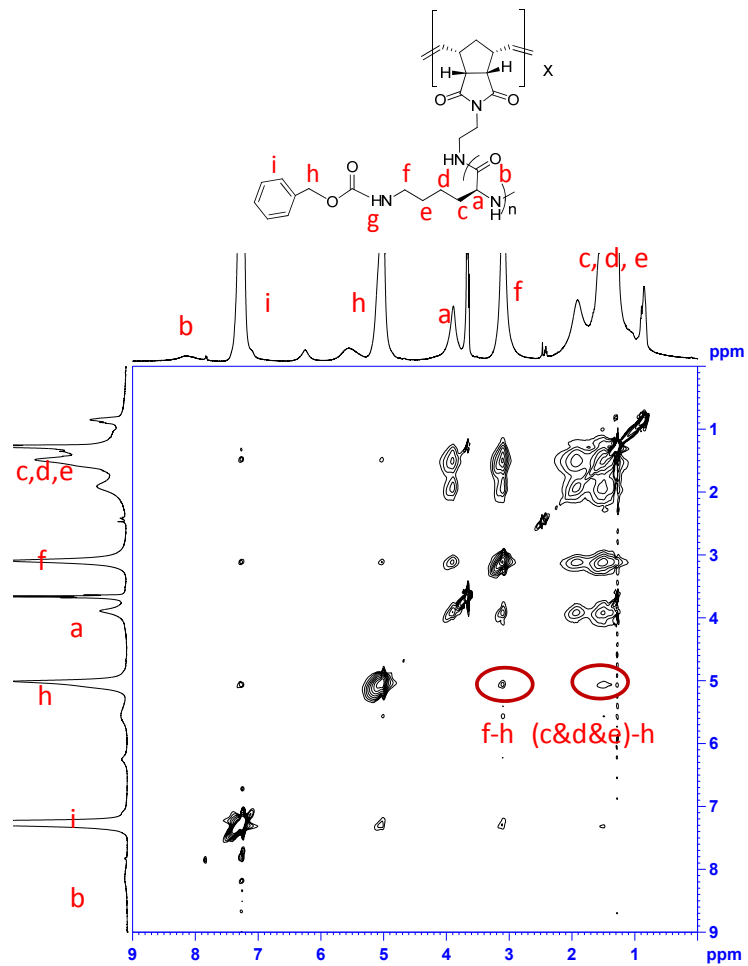


Figure S33. The NOESY spectrum of $(PN-g-PZLL_{50})_x$ obtained by using the $(\pi/2)-t_1-(\pi/2)-\tau_m-(\pi/2)-t_2$ pulse sequence.

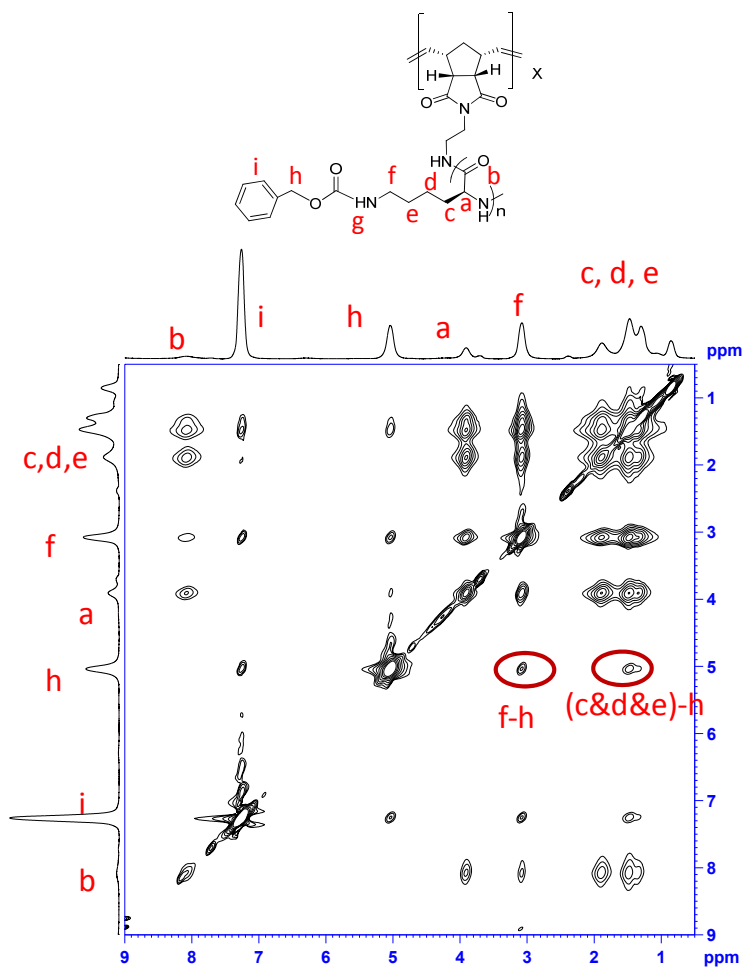


Figure S34. The NOESY spectrum of $(\text{PN-g-PZLL}_{57})_{10}$ obtained by using the $(\pi/2)-t_1-(\pi/2)-\tau_m-(\pi/2)-t_2$ pulse sequence.

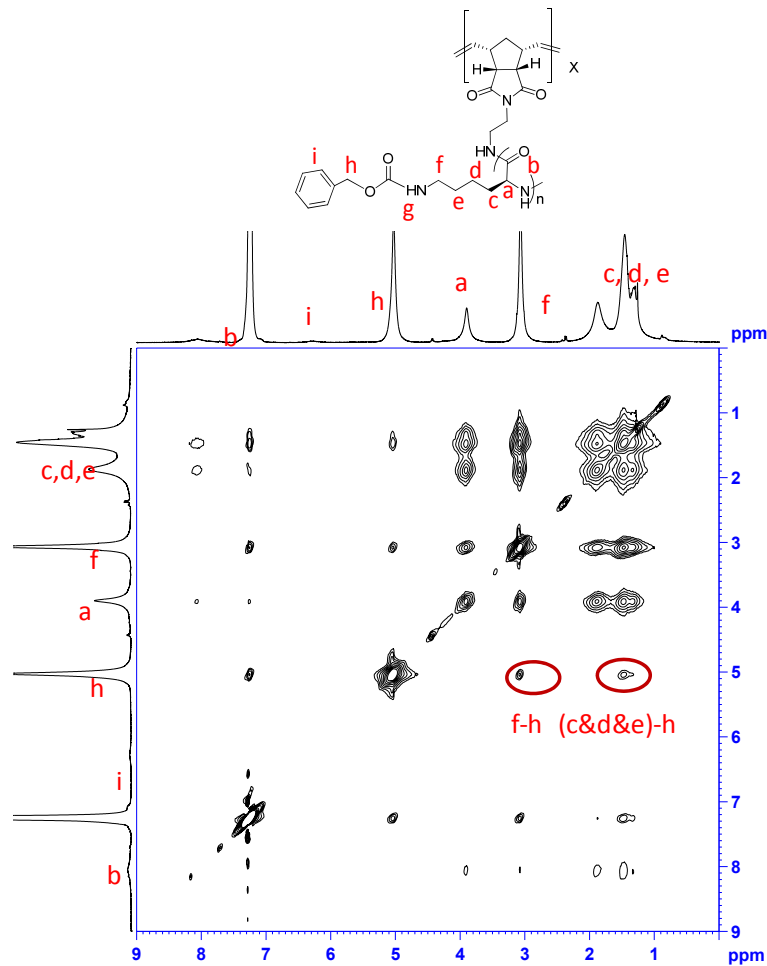


Figure S35. The NOESY spectrum of (PN-g-PZLL₆₇)₁₀ obtained by using the $(\pi/2)$ - t_1 - $(\pi/2)$ - τ_m - $(\pi/2)$ - t_2 pulse sequence.

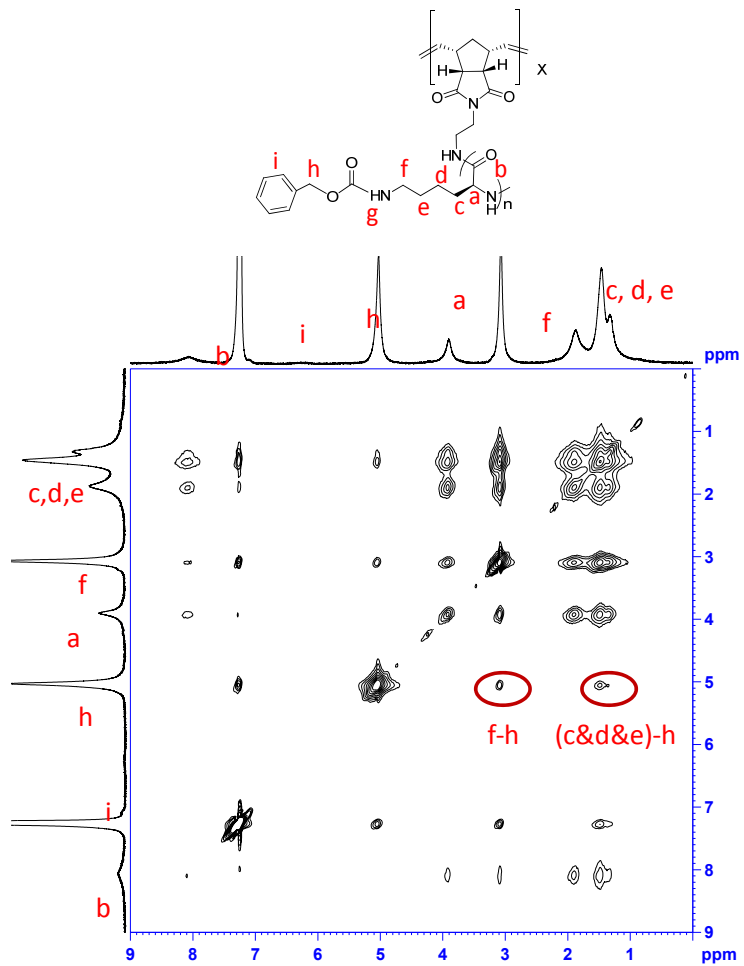


Figure S36. The NOESY spectrum of $(\text{PN-g-PZLL}_{70})_9$ obtained by using the $(\pi/2)-t_1-(\pi/2)-\tau_m-(\pi/2)-t_2$ pulse sequence.

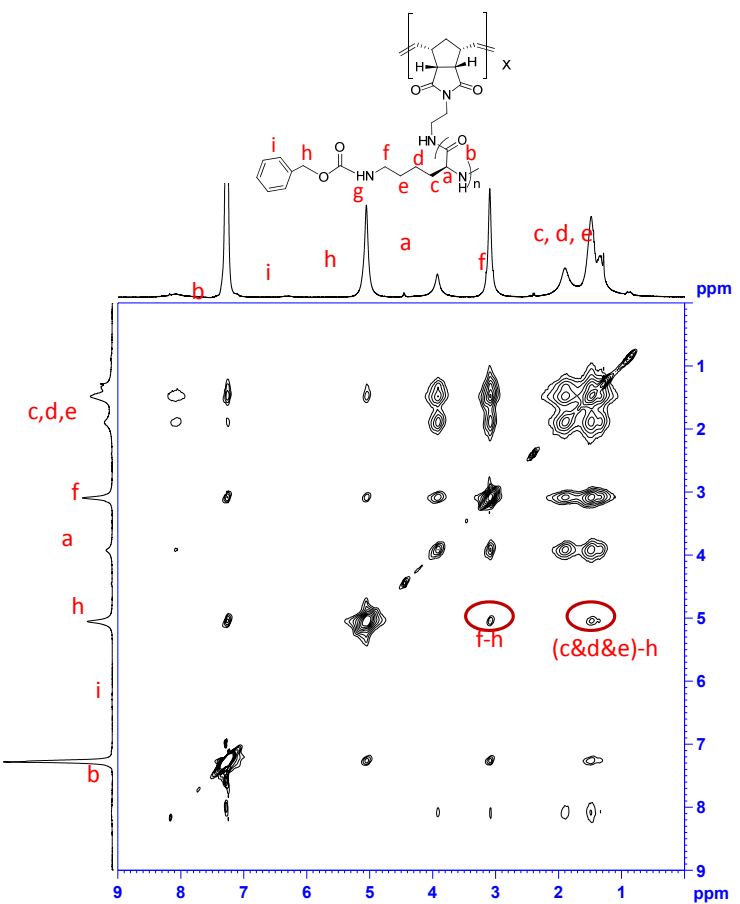


Figure S37. The NOESY spectrum of $(\text{PN-g-PZLL}_{95})_{10}$ obtained by using the $(\pi/2)-t_1-(\pi/2)-\tau_m-(\pi/2)-t_2$ pulse sequence.

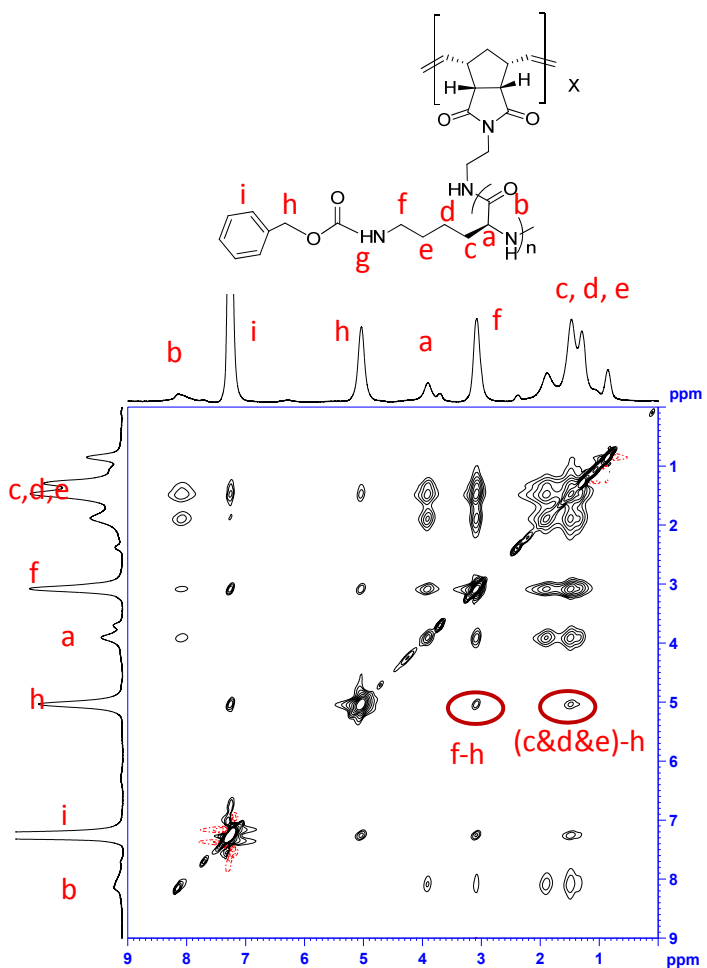


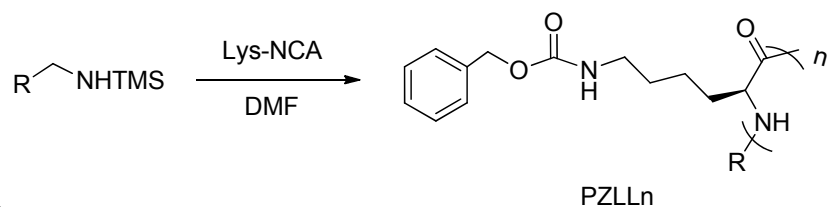
Figure S38. The NOESY spectrum of $(PN-g-PZLL_{122})_{10}$ obtained by using the $(\pi/2)-t_1-(\pi/2)-\tau_m-(\pi/2)-t_2$ pulse sequence.

Table S1 The normalized intensities of specific cross peaks in NOESY spectra obtained from the brush-like polymers with different grafted PBLG lengths and grafting densities. The intensity of the cross peak arising from the resonances between α -proton and β - & γ -protons were used for the normalization.

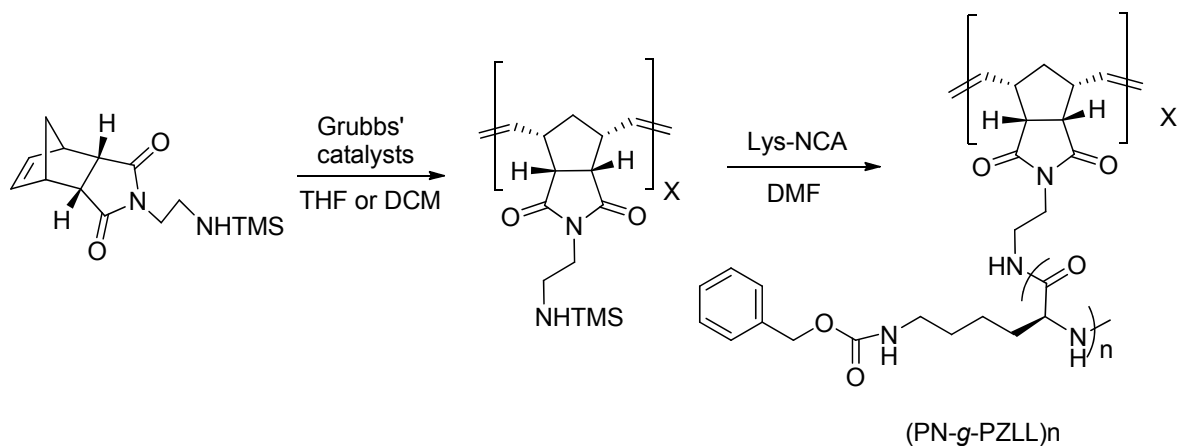
	DP of grafted PBLG	$S_{\text{grafted-}}_{\text{PBLG}} / S_{\text{PBLG}}$	V_{f-e} $/V_{a-d\&c}$	V_{f-a} $/V_{a-d\&c}$	$V_{f-d\&c}$ $/V_{a-d\&c}$	V_{e-a} $/V_{a-d\&c}$	$V_{e-d\&c}$ $/V_{a-d\&c}$
(PN- <i>g</i> -PBLG ₅₀) ₁₇	50	0.82	0.09	0.04	0.20	0.05	0.26
(PN- <i>g</i> -PBLG ₁₄₅) ₁₈	145	0.54	0.61	0.14	0.95	0.15	0.68
(PN- <i>g</i> -PBLG ₉₁) ₂₃ -r-Pn ₅₈	91	0.65	0.25	0.08	0.46	0.12	0.40
(PN- <i>g</i> -PBLG ₇₆) ₈ -r-Pn ₆₀	76	0.92	0.03	0.02	0.09	0.02	0.12
(PN- <i>g</i> -PBLG ₁₁₉) ₈ -r-Pn ₆₀	119	0.77	0.17	0.05	0.35	0.06	0.30
PBLG ₅₁	51	1.00	0.02	0.01	0.05	0.02	0.08

Scheme S1. Controlled NCA polymerizations of PZLL and PN-*g*-PZLL

A.



B.



Appendix. A Mathematica® file (***apparent cooperativity.nb***) is attached in the end of the SI. It shows how the apparent cooperativity (S) and the number of residues (n) are correlated, based on Zimm-Bragg's model².

Reference

1. Goodman, M. & Masuda, M. *Biopolymers* **2**, 107 (1964).
2. Zimm, B. H. & Bragg, J. K. *J. Chem. Phys.* **31**, 526 (1959).

Appendix: Apparent Cooperativity.nb | This *Mathematica* file uses Zimm-Bragg model to derive the apparent cooperativity (S) as a function of the number of residues (n) and the helix parameter σ , by taking the partial derivative of fractional helicity (θ) with respect to s at the midpoint of the helix-coil transition, at which s has a critical value of unity. The dependence of S on n is then evaluated at $\sigma=0.0001$ (a reasonable value for PBLG in the environmental conditions used in the study).

```

ClearAll[\theta, s, \sigma, \lambda1, \lambda2, n, s, q, f]

\lambda1 := ((1 + s) + ((1 - s)^2 + 4 * \sigma * s)^0.5) * 0.5
\lambda2 := ((1 + s) - ((1 - s)^2 + 4 * \sigma * s)^0.5) * 0.5
q := (\lambda1^(n + 1) * (1 - \lambda2) - \lambda2^(n + 1) * (1 - \lambda1)) / (\lambda1 - \lambda2)
\theta := s / (n * q) * D[q, s]
S = Simplify[D[\theta, s]]

```

$$\left(e^{1.38629 n} \right.$$

$$\left(- \left(0.5^n s \left(0. + 1. \left(1 - 2 s + s^2 + 4 s \sigma \right)^{0.5} \right) \left(0.25 \left(1 + (-1. + 1. s + 2. \sigma) / (1 - 2 s + s^2 + 4 s \sigma)^{0.5} \right)^{1+n} + 0.5 (1 + n) \left(1 + (-1. + 1. s + 2. \sigma) / (1 - 2 s + s^2 + 4 s \sigma)^{0.5} \right) \left(0.5 - 0.5 s + 0.5 \left(1 - 2 s + s^2 + 4 s \sigma \right)^{0.5} \right) \left(1 + s + \left(1 - 2 s + s^2 + 4 s \sigma \right)^{0.5} \right)^n - 0.25 \left(1 + (1. - 1. s - 2. \sigma) / (1 - 2 s + s^2 + 4 s \sigma)^{0.5} \right) \left(1 + s + \left(1 - 2 s + s^2 + 4 s \sigma \right)^{0.5} \right)^{1+n} - 0.5 (1 + n) \left(1 + (1. - 1. s - 2. \sigma) / (1 - 2 s + s^2 + 4 s \sigma)^{0.5} \right) \left(1 + s - \left(1 - 2 s + s^2 + 4 s \sigma \right)^{0.5} \right)^n \left(1 - 0.5 \left(1 + s + \left(1 + s^2 + s (-2 + 4 \sigma) \right)^{0.5} \right) \right) \right) \right)$$

$$\left(0.5^n \left(0. + 1. \left(1 - 2 s + s^2 + 4 s \sigma \right)^{0.5} \right) \left(0.25 \left(1 + (-1. + 1. s + 2. \sigma) / (1 - 2 s + s^2 + 4 s \sigma)^{0.5} \right)^{1+n} + 0.5 (1 + n) \left(1 + (-1. + 1. s + 2. \sigma) / (1 - 2 s + s^2 + 4 s \sigma)^{0.5} \right) \left(0.5 - 0.5 s + 0.5 \left(1 - 2 s + s^2 + 4 s \sigma \right)^{0.5} \right) \left(1 + s + \left(1 - 2 s + s^2 + 4 s \sigma \right)^{0.5} \right)^n - 0.25 \left(1 + (1. - 1. s - 2. \sigma) / (1 - 2 s + s^2 + 4 s \sigma)^{0.5} \right) \left(1 + s + \left(1 - 2 s + s^2 + 4 s \sigma \right)^{0.5} \right)^{1+n} - 0.5 (1 + n) \left(1 + (1. - 1. s - 2. \sigma) / (1 - 2 s + s^2 + 4 s \sigma)^{0.5} \right) \left(1 + s - \left(1 - 2 s + s^2 + 4 s \sigma \right)^{0.5} \right)^n \left(1 - 0.5 \left(1 + s + \left(1 + s^2 + s (-2 + 4 \sigma) \right)^{0.5} \right) \right) \right) \right)$$

$$\left(0.5^n (-1. + 1. s + 2. \sigma) \left(0.5 \left(0.5 - 0.5 s + 0.5 \left(1 - 2 s + s^2 + 4 s \sigma \right)^{0.5} \right) \left(1 + s + \left(1 - 2 s + s^2 + 4 s \sigma \right)^{0.5} \right)^{1+n} - 0.5 \left(1 + s - \left(1 - 2 s + s^2 + 4 s \sigma \right)^{0.5} \right)^{1+n} \right) \right.$$

$$\begin{aligned}
& \frac{1}{(1 - 2s + s^2 + 4s\sigma)^{0.5}} \cdot 0.5^n (-1. + 1. s + 2. \sigma) \\
& \left(0.5 \left(0.5 - 0.5s + 0.5 (1 - 2s + s^2 + 4s\sigma)^{0.5} \right) \left(1 + s + (1 - 2s + s^2 + 4s\sigma)^{0.5} \right)^{1+n} - \right. \\
& \quad 0.5 \left(1 + s - (1 - 2s + s^2 + 4s\sigma)^{0.5} \right)^{1+n} \\
& \quad \left. \left(1 - 0.5 \left(1 + s + (1 + s^2 + s(-2 + 4\sigma))^{0.5} \right) \right) \right) \Bigg) \\
& \left(0. + 1. (1 - 2s + s^2 + 4s\sigma)^{1.5} \right) + \left(0.5^n s \left(0. + 1. (1 - 2s + s^2 + 4s\sigma)^{0.5} \right) \right. \\
& \quad \left(0.5 \left(0.5 - 0.5s + 0.5 (1 - 2s + s^2 + 4s\sigma)^{0.5} \right) \left(1 + s + (1 - 2s + s^2 + 4s\sigma)^{0.5} \right)^{1+n} - \right. \\
& \quad \left. 0.5 \left(1 + s - (1 - 2s + s^2 + 4s\sigma)^{0.5} \right)^{1+n} \left(1 - 0.5 \left(1 + s + (1 + s^2 + s(-2 + 4\sigma))^{0.5} \right) \right) \right) \\
& \left(0.5^n \left(0. + 1. (1 - 2s + s^2 + 4s\sigma)^{1.} \right) \right. \\
& \quad \left(0.5 (1+n) \left(1 + (1. - 1. s - 2. \sigma) / (1 - 2s + s^2 + 4s\sigma)^{0.5} \right) \left(1 + (-1. + 1. s + \right. \right. \\
& \quad \left. \left. 2. \sigma) / (1 - 2s + s^2 + 4s\sigma)^{0.5} \right) \left(1 + s - (1 - 2s + s^2 + 4s\sigma)^{0.5} \right)^n + \right. \\
& \quad 0.25 \left(- (1. (-1. + s + 2. \sigma)^2) / (1 - 2s + s^2 + 4s\sigma)^{1.5} + \right. \\
& \quad \left. 1. / (1 - 2s + s^2 + 4s\sigma)^{0.5} \right) \left(1 + s - (1 - 2s + s^2 + 4s\sigma)^{0.5} \right)^{1+n} + \right. \\
& \quad 0.5 n (1+n) \left(1 + (-1. + 1. s + 2. \sigma) / (1 - 2s + s^2 + 4s\sigma)^{0.5} \right)^2 \\
& \quad \left(0.5 - 0.5s + 0.5 (1 - 2s + s^2 + 4s\sigma)^{0.5} \right) \left(1 + s + (1 - 2s + s^2 + 4s\sigma)^{0.5} \right)^{-1+n} - \\
& \quad 0.5 (1+n) \left(1 + (1. - 1. s - 2. \sigma) / (1 - 2s + s^2 + 4s\sigma)^{0.5} \right) \\
& \quad \left(1 + (-1. + 1. s + 2. \sigma) / (1 - 2s + s^2 + 4s\sigma)^{0.5} \right) \\
& \quad \left(1 + s + (1 - 2s + s^2 + 4s\sigma)^{0.5} \right)^n + 0.5 (1+n) \left(- (1. (-1. + s + 2. \sigma)^2) / \right. \\
& \quad \left. (1 - 2s + s^2 + 4s\sigma)^{1.5} + 1. / (1 - 2s + s^2 + 4s\sigma)^{0.5} \right) \\
& \quad \left(0.5 - 0.5s + 0.5 (1 - 2s + s^2 + 4s\sigma)^{0.5} \right) \left(1 + s + (1 - 2s + s^2 + 4s\sigma)^{0.5} \right)^n - \\
& \quad 0.25 \left((1. (-1. + s + 2. \sigma)^2) / (1 - 2s + s^2 + 4s\sigma)^{1.5} - \right. \\
& \quad \left. 1. / (1 - 2s + s^2 + 4s\sigma)^{0.5} \right) \left(1 + s + (1 - 2s + s^2 + 4s\sigma)^{0.5} \right)^{1+n} - \\
& \quad 0.5 n (1+n) \left(1 + (1. - 1. s - 2. \sigma) / (1 - 2s + s^2 + 4s\sigma)^{0.5} \right)^2 \\
& \quad \left(1 + s - (1 - 2s + s^2 + 4s\sigma)^{0.5} \right)^{-1+n} \left(1 - 0.5 \left(1 + s + (1 + s^2 + s(-2 + 4\sigma))^{0.5} \right) \right) - \\
& \quad 0.5 (1+n) \left((1. (-1. + s + 2. \sigma)^2) / (1 - 2s + s^2 + 4s\sigma)^{1.5} - \right. \\
& \quad \left. 1. / (1 - 2s + s^2 + 4s\sigma)^{0.5} \right) \left(1 + s - (1 - 2s + s^2 + 4s\sigma)^{0.5} \right)^n \\
& \quad \left(1 - 0.5 \left(1 + s + (1 + s^2 + s(-2 + 4\sigma))^{0.5} \right) \right) - 1 / (1 - 2s + s^2 + 4s\sigma)^{0.5} \\
& \quad 2 \times 0.5^n (-1. + 1. s + 2. \sigma) \left(0. + 1. (1 - 2s + s^2 + 4s\sigma)^{0.5} \right) \\
& \quad \left(0.25 \left(1 + (-1. + 1. s + 2. \sigma) / (1 - 2s + s^2 + 4s\sigma)^{0.5} \right) \right)
\end{aligned}$$

$$\begin{aligned}
& \left(1 + s - (1 - 2s + s^2 + 4s\sigma)^{0.5} \right)^{1+n} + \\
& 0.5 (1+n) \left(1 + (-1. + 1.s + 2.\sigma) / (1 - 2s + s^2 + 4s\sigma)^{0.5} \right) \\
& \left(0.5 - 0.5s + 0.5 (1 - 2s + s^2 + 4s\sigma)^{0.5} \right) \left(1 + s + (1 - 2s + s^2 + 4s\sigma)^{0.5} \right)^n - \\
& 0.25 \left(1 + (1. - 1.s - 2.\sigma) / (1 - 2s + s^2 + 4s\sigma)^{0.5} \right) \\
& \left(1 + s + (1 - 2s + s^2 + 4s\sigma)^{0.5} \right)^{1+n} - \\
& 0.5 (1+n) \left(1 + (1. - 1.s - 2.\sigma) / (1 - 2s + s^2 + 4s\sigma)^{0.5} \right) \\
& \left(1 + s - (1 - 2s + s^2 + 4s\sigma)^{0.5} \right)^n \left(1 - 0.5 \left(1 + s + (1 + s^2 + s(-2 + 4\sigma))^{0.5} \right) \right) + \\
& 1 / \left(1 - 2s + s^2 + 4s\sigma \right)^{1.} - 2 \times 0.5^n (1. - 1.s - 2.\sigma)^2 \\
& \left(0.5 \left(0.5 - 0.5s + 0.5 (1 - 2s + s^2 + 4s\sigma)^{0.5} \right) \left(1 + s + (1 - 2s + s^2 + 4s\sigma)^{0.5} \right)^{1+n} - \right. \\
& 0.5 \left(1 + s - (1 - 2s + s^2 + 4s\sigma)^{0.5} \right)^{1+n} \\
& \left. \left(1 - 0.5 \left(1 + s + (1 + s^2 + s(-2 + 4\sigma))^{0.5} \right) \right) \right) - \\
& 0.5^n \left(0. + 1. \left(1 - 2s + s^2 + 4s\sigma \right)^{0.5} \right) \left(-0.5 \left((1. (-1. + s + 2.\sigma)^2) / \right. \right. \\
& \left. \left. (1 - 2s + s^2 + 4s\sigma)^{1.5} - 1. / (1 - 2s + s^2 + 4s\sigma)^{0.5} \right) + \right. \\
& 0.5 \left(- (1. (-1. + s + 2.\sigma)^2) / (1 - 2s + s^2 + 4s\sigma)^{1.5} + 1. / \right. \\
& \left. \left. (1 - 2s + s^2 + 4s\sigma)^{0.5} \right) \right) \left(0.5 \left(0.5 - 0.5s + 0.5 (1 - 2s + s^2 + 4s\sigma)^{0.5} \right)^{1+n} \right. \\
& \left. \left(1 + s + (1 - 2s + s^2 + 4s\sigma)^{0.5} \right)^{1+n} - 0.5 \left(1 + s - (1 - 2s + s^2 + 4s\sigma)^{0.5} \right)^{1+n} \right. \\
& \left. \left(1 - 0.5 \left(1 + s + (1 + s^2 + s(-2 + 4\sigma))^{0.5} \right) \right) \right) \Bigg) / \\
& \left(0. + 1. \left(1 - 2s + s^2 + 4s\sigma \right)^{1.5} \right) \Bigg) / \left(n \right. \\
& \left. \left(0.5 \left(0.5 - 0.5s + 0.5 (1 - 2s + s^2 + 4s\sigma)^{0.5} \right)^{1+n} \right. \right. \\
& \left. \left(1 + s + (1 - 2s + s^2 + 4s\sigma)^{0.5} \right)^{1+n} - \right. \\
& \left. 0.5 \left(1 + s - (1 - 2s + s^2 + 4s\sigma)^{0.5} \right)^{1+n} \right. \\
& \left. \left(1 - 0.5 \left(1 + s + (1 + s^2 + s(-2 + 4\sigma))^{0.5} \right) \right) \right)^2 \Bigg)
\end{aligned}$$

s = 1

1

f[n_] = Simplify[s]

```
 $\sigma = 0.0001$ 
Plot[f[n], {n, 0, 200}, PlotRange -> Automatic]
```

0.0001

